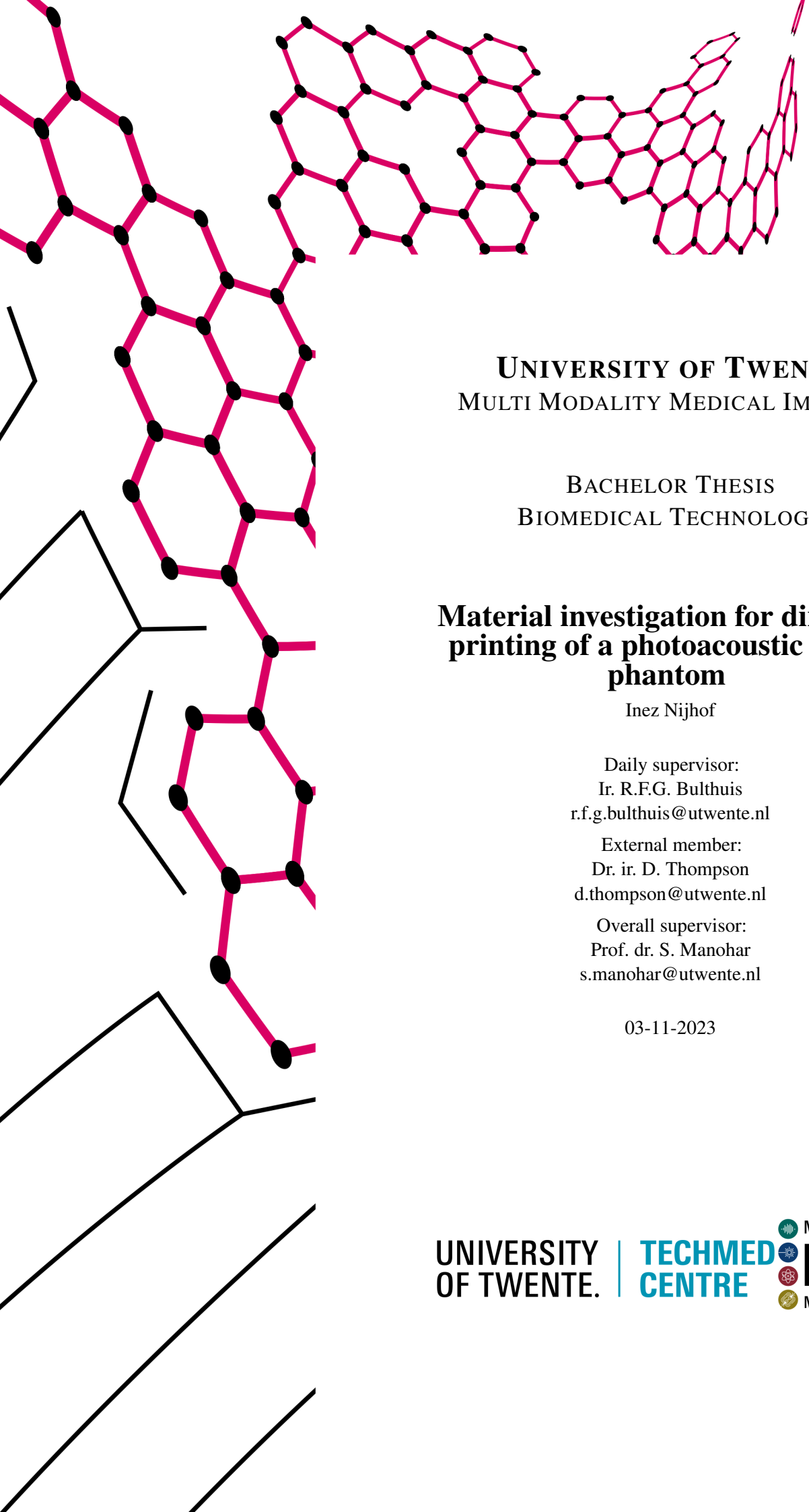

UNIVERSITY OF TWENTE
MULTI MODALITY MEDICAL IMAGING

BACHELOR THESIS
BIOMEDICAL TECHNOLOGY

Material investigation for direct 3D printing of a photoacoustic breast phantom

Inez Nijhof

Daily supervisor:
Ir. R.F.G. Bulthuis
r.f.g.bulthuis@utwente.nl

External member:
Dr. ir. D. Thompson
d.thompson@utwente.nl

Overall supervisor:
Prof. dr. S. Manohar
s.manohar@utwente.nl

03-11-2023

UNIVERSITY OF TWENTE. | TECHMED CENTRE | Multi-Modality M3i Medical Imaging

Abstract

Breast cancer is a global health concern, and photoacoustic imaging offers a promising technique for breast cancer detection. To improve photoacoustic breast imaging, investigations on realistic breast phantoms are essential. Currently, copolymer-in-oil has been chosen by the Internation Photoacousic community as the optimum material for making phantoms. Traditionally phantoms are made by casting into mould, but direct 3D printing of phantoms is being investigated by the University of Twente. However, the material needs adjustments to match breast tissue's optical and acoustic properties accurately. This study addresses the question of how to improve the copolymer-in-oil recipe to create a more realistic breast tissue-mimicking material suitable for 3D printing.

The study began by exploring dyes for the absorption coefficient (μ_a), with yellow wax showing potential for replicating breast tissue's (μ_a). The exact concentration of yellow wax requires fine-tuning. The copolymer-in-oil recipe was prepared, revealing challenges related to temperature control and material consistency. Adjustments to one of the consitituents' (LDPE) concentration is needed to align the material's speed of sound with that of breast tissue. Further research should determine the optimal LDPE concentration.

Optical characterization demonstrated deviations in μ_a spectra, primarily due to yellow wax. The choice of method for measuring the speed of sound showed variations between peak and threshold-based approaches. Thermal analysis indicated the material's potential suitability for 3D printing.

In conclusion, further refinements are required for the copolymer-in-oil recipe to achieve a realistic breast tissue-mimicking material suitable for 3D bio-printing. These adjustments should address both optical and acoustic properties. This research provides a foundation for improving copolymer-in-oil as a phantom material for advanced breast imaging techniques, contributing to the field of medical diagnostics and imaging.

Samenvatting

Borstkanker is een wereldwijd gezondheidsprobleem, en fotoakoestische beeldvorming biedt een veelbelovende techniek voor de detectie van borstkanker. Om fotoakoestische borstbeeldvorming te verbeteren, zijn onderzoeken met realistische borstfantomen essentieel. Momenteel is door de internationale fotoakoestische gemeenschap gekozen voor copolymeer-in-olie als het optimale materiaal voor het maken van fantomen. Traditioneel worden fantomen gegoten in mallen, maar de directe 3D-printing van fantomen wordt onderzocht door de Universiteit Twente. Het materiaal heeft echter aanpassingen nodig om nauwkeurig overeen te komen met de optische en akoestische eigenschappen van borstweefsel. Deze studie behandelt de vraag hoe het copolymeer-in-olie recept verbeterd kan worden om een realistischer materiaal te creëren dat geschikt is voor 3D-printen en lijkt op borstweefsel.
De studie begon met het verkennen van kleurstoffen voor de absorptiecoëfficiënt (μ_a), waarbij geel was een potentieel vertoonde om de (μ_a) van borstweefsel na te bootsen. De exacte concentratie van gele was vereist fijnafstemming. Het copolymeer-in-olie recept werd bereid, waarbij uitdagingen werden geïdentificeerd met betrekking tot temperatuurregeling en materiaalconsistentie. Aanpassingen aan de concentratie van een van de bestanddelen (LDPE) zijn nodig om de snelheid van geluid van het materiaal af te stemmen op die van borstweefsel. Verder onderzoek moet de optimale LDPE-concentratie bepalen.
Optische karakterisering toonde afwijkingen in μ_a-spectra, voornamelijk als gevolg van gele was. De keuze van de methode voor het meten van de geluidssnelheid vertoonde variaties tussen piek- en drempelgebaseerde benaderingen. Thermische analyse gaf aan dat het materiaal potentieel geschikt is voor 3D-printen.
Samengevat zijn verdere verfijningen nodig voor het copolymeer-in-olie recept om een realistisch materiaal te creëren dat geschikt is voor 3D-bioprinten en lijkt op borstweefsel. Deze aanpassingen moeten zowel optische als akoestische eigenschappen aanpakken. Dit onderzoek legt een basis voor het verbeteren van copolymeer-in-olie als fantoommateriaal voor geavanceerde borstbeeldvormingstechnieken, wat bijdraagt aan het vakgebied van medische diagnostiek en beeldvorming.

Contents

1 Introduction

The most common cancer diagnosed worldwide and one of the leading causes of cancer death in females is breast cancer [1]. Photoacoustic imaging is a promising technique which can image the characteristics of breast cancer [2]. These characteristics are an increase in blood vessel density and a decrease in oxyhemoglobin concentration [3]. In collaboration with European partners, the University of Twente has been developing an advanced photoacoustic breast imaging system; photoacoustic mammography 3 (PAM3) [4, 5].

To characterize and calibrate photoacoustic and ultrasound breast tomography setups, such as the PAM3, realistic breast phantoms are essential. Current methods rely on molding techniques [6] which, unfortunately, are time-consuming and face challenges when creating small structures. An alternative approach is 3D printing, holding promise for crafting intricate structures.
The material currently used in the molding technique for creating phantoms is gel wax. The advantage of this material is the tuneability for optical and acoustic properties, has high stability, and is mechanical robust. Additionally, it is also suitable for photoacoustic imaging. The gel wax could even be used for directly 3D printing [7]. Initial tests have shown promise in 3D printing a soft material known as copolymer-in-oil. These experiments have displayed its ability to provide adjustable properties, effectively mimicking biological tissues, especially within the optical and acoustic ranges crucial for biomedical photoacoustic imaging. Moreover, these tests have confirmed that this material maintains its photoacoustic, thermomechanical, and longitudinal stability, making it suitable for both short-term and long-term precision studies [8].

Creating a stable phantom material suitable for optical and acoustic imaging involves developing a 3D-printable photoacoustic breast phantom using a copolymer-in-oil composition. However, this material currently does not entirely align with the optical and acoustic properties of breast tissue, specifically in relation to fatty and fibroglandular tissue. The difference presents difficulties in attaining an accurate and precise depiction within photoacoustic breast imaging phantoms. To address this issue, a potential solution lies in modifying the copolymer-in-oil recipe. By adjusting the additives to closely match the optical spectrum of breast tissue and modifying the concentration of the base components to closely match the acoustic spectrum of breast tissue. This will enable a more accurate and realistic phantom for research applications.

This leads to the following research question: "*How can the recipe of copolymer-in-oil phantom material be improved to match the optical and acoustic properties of breast tissue, specifically fatty and fibroglandular tissue, to create a more realistic and accurate breast tissue-mimicking material that is potentially suitable for 3D printing?*". The following sub-questions must be answered to tackle the research question:

- "*What are the specific optical and acoustic properties of both fatty and fibroglandular breast tissues that need to be replicated in the phantom material?*"
- "*What adjustments are required to the copolymer-in-oil recipe to improve its optical properties, such as absorption and scattering coefficients, to better match those of breast tissue?*"
- "*What adjustments are required to the copolymer-in-oil recipe to improve its acoustic properties, such as sound speed and attenuation, to better match those of breast tissue?*"
- "*Is the improved recipe potentially suitable for 3D printing?*"

To enhance the development and optimization of setups like the PAM3, the use of standardized materials is imperative. Currently, the molding technique employed is both time-consuming and poses challenges when dealing with small structures. An alternative approach, 3D printing, holds promise; however, the available material lacks sufficient data. By conducting a comprehensive study on breast tissue properties, including its diverse optical and acoustic characteristics, it becomes possible to fine-tune the copolymer-in-oil material. This adjustment will enhance the realism of directly 3D-printed phantoms, thereby contributing to the testing and improvement of photoacoustic and ultrasound breast tomography setups.

Section 2 provides an overview of the literature on the operation of photoacoustic imaging, the existing material and the properties of breast tissue. The requirements and wishes for the material and the phantom can be

seen in Section 3. The method for determining a dye for the absorption coefficient, making the material and characterising the optical, acoustic and thermal properties can be seen in Section 4. Following this, Section 5 discusses the key findings. Based on the results, the discussion, and conclusion and outlook are presented in Sections 6 and 7. The method, results and discussion are all divided in different sections. The first one is for determining the dye for the absorption coefficient, the second one is for making the copolymer-in-oil and the last one is for the characterisation of the copolymer-in-oil. This last section is also divided in three more subsections; the optical characterisation, the acoustic characterisation and the thermo analysis.

2 Background theory

2.1 Photoacoustic Imaging

Photoacoustic (PA) imaging enables the visualization of deep optical absorption in tissue with high resolution [3]. This technique makes it possible to reveal the optical absorption contrast related to the formation of blood vessels and tumours associated with angiogenesis [3]. For patients, PA imaging is user-friendly, as it requires neither breast compression, nor any potentially harmful radiation, nor a contrast agent [10].
An overview of the PA process can be seen in Figure 1. The entire process is divided into three steps: the optical process, the photoacoustic effect and the acoustic process [9]. The optical process starts with a short-pulsed light source, near-infrared. It is used for illuminating the tissue [2]. The light is selectively absorbed in regions with higher absorption when the tissue is heated by the light source, this is the photoacoustic effect. The absorbed optical energy ($H(r)$), from the optical process, rapidly undergoes thermalization. The thermalization leads to a thermoelastic expansion, which causes an initial pressure ($p_0(r)$), which can be detected with an ultrasound (US) transducer from the acoustic process. The absorbed optical energy ($H(r)$) and the initial pressure ($p_0(r)$) are given by the following equations:

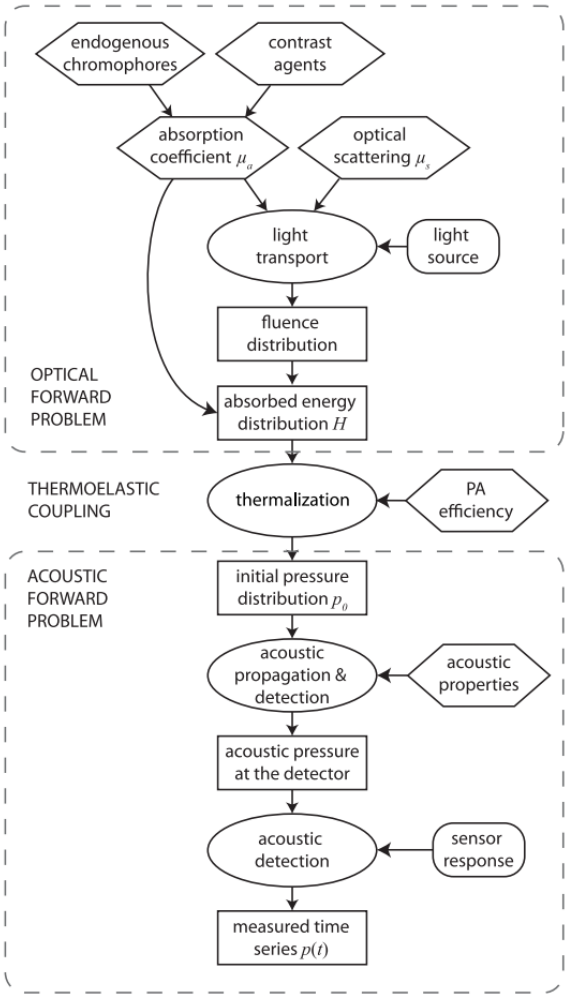

Figure 1: An overview of the photoacoustic process [9].

$$H(r) = \mu_a(r)\phi(r) \tag{1}$$

$$p_0(r) = \frac{\beta C_s^2}{C_p} H(r) = \Gamma H(r) \tag{2}$$

The product of the light fluence ($\phi(r)$) of the absorber and the absorption coefficient (μ_a) give the absorbed optical energy ($H(r)$). The initial pressure ($p_0(r)$) that is generated is the product of $H(r)$ and the Grüneisen coefficient (Γ). β is the isobaric thermal expansion coefficient, C_s is the speed of sound and C_p is the isobaric specific heat capacity [3].

2.2 Copolymer-in-oil

Copolymer-in-oil is a material that can be independently tuned for the optical and acoustic properties. It is also suitable for making phantoms for PA imaging. Our ambition is to make it match with the properties of breast tissue and 3D print breast phantoms using it. The foundational material comprises mineral oil, styrene-ethylene/butylene-styrene (SEBS) and Low-density Polyethylene (LDPE) [11].
SEBS is a copolymer consisting of three polymers: styrene, ethylene and butylene. These monomers are arranged in blocks within the polymer structure, and this gives SEBS its unique combination of properties. Butylene, as the comonomer, gives the copolymer high strength and is easily processed [12]. The structure of the copolymer can be seen in Figure 2.
LDPE is a type of polyethylene. It has a low density and consists of an irregular structure of polymer chains with many branches and short branches. These branches result in a more flexible material. Since the material is a suitable strengthening agent, Hacker et al. proceed to work further with LDPE instead of other variations of polyethylene [13].
By changing the titanium dioxide (TiO_2) and the oil-soluble dye concentration the reduced scattering coefficient (μ_s') and μ_a can be tuned respectively [13]. An increase in the TiO_2 concentration leads to an increase in the μ_s'. An increase in the oil-soluble dye concentration, in this case Nigrosin, leads to an increase in the μ_a [8]. The acoustic properties are connected to the base materials [14]. The speed of sound can be increased by adding paraffin wax or glycerol to the material. The disadvantage of these components is that their addition causes higher acoustic attenuation or backscattering to the material [8]. When changing the concentration of LDPE, you do change the speed of sound which does not cause backscattering [8]. The benefit of copolymer-in-oil lies in its cost-effectiveness, its non-water absorption properties, its non-toxic nature, and biological inertness [8]. Because of its easily replaceable manufacturing process, robustness, and its alignment with biologically significant characteristics, the material equation shows considerable potential in efforts aimed at establishing multi modal acoustic-optical standards [13].

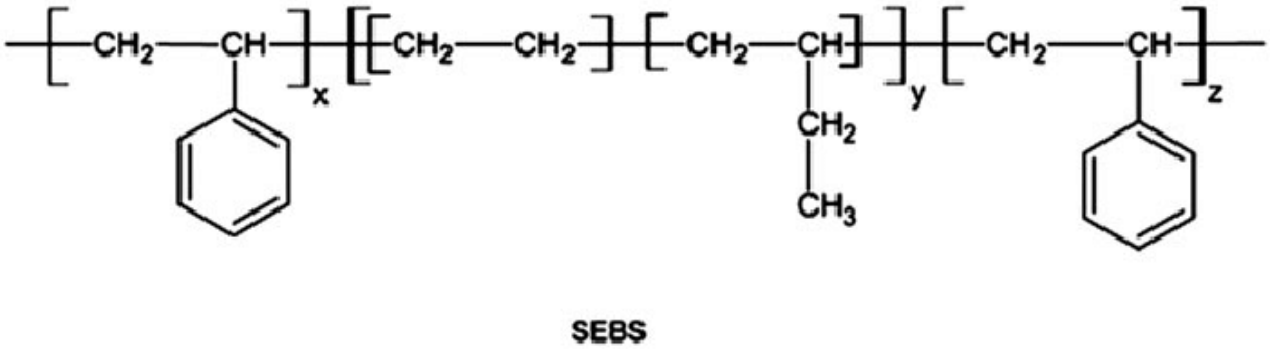

SEBS

Figure 2: The structure of SEBS [12]. The different monomers can be seen in this figure. From left to right: styrene, ethylene, butylene and styrene.

2.3 The female breast

2.3.1 Anatomy

The female breast, covered by the skin, rests atop the pectoral muscle within the chest wall. Internally, it comprises 15-25 glandular lobules radiating around the nipple, enveloped by fibrous and fatty tissue. Each lobe is drained by a duct, itself consisting of 20-40 smaller lobules. These lobules, approximately 1-2 mm in diameter, contain a complex network of tiny ducts capable of hormonal stimulation to produce milk, terminating in blind endings. Collectively, these ducts merge into approximately 5 to 10 major ducts that ultimately lead to the nipple [15]. This structure can be seen in Figure 3.
The proportion of fatty and fibroglandular tissue varies among individuals and can also change with Body Mass Index (BMI), pregnancy and hormonal factors such as age [6]. For example, breast tissue in women under 50 years of age contains significantly higher concentrations of fibroglandular tissue compared to that in older women.
Conversely, lipid concentration is lower in women under 50 years of age and higher in women over 50 years of age. Furthermore, the amounts of water and collagen decrease in women with a higher BMI, while the amount of lipids increases [16].

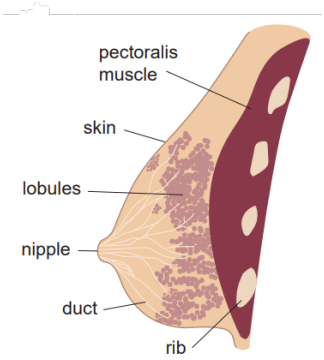

Figure 3: Anatomy of the human breast [15].

2.3.2 Optical properties

The optical properties of healthy human breast tissue can be seen in Figure 4, the blue line represents the fibroglandular tissue, the red line the fatty tissue and the green line a mixture of the fatty and fibroglandular tissue. The data from Faroni et al. [17] is obtained with time-resolved diffuse spectroscopy measuring in vivo from the breasts of three healthy volunteers with different breast types.

The absorption spectrum of copolymer-in-oil (12 w/w% SEBS and 5 w/w% LDPE) that is measured with a double integrated sphere by the Institut für Lasertechnologien in der Medizin und Meßtechnik an der Universität Ulm [18]. The fatty and fibroglandular tissue breast tissue [17] are subtracted from the Ulm sample to get the spectrum of the desired additive for μ_a. This can be seen in Figure 5. Furthermore, in this paper, the sample and measurements done by der Universität Ulm, are referred to as the Ulm sample/measurements.

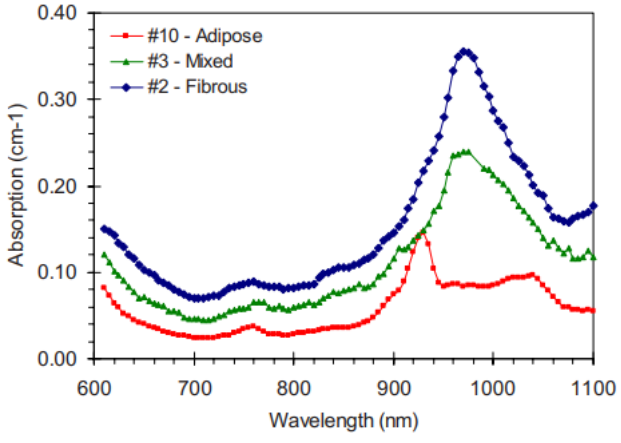

(a) Absorption spectra [17]

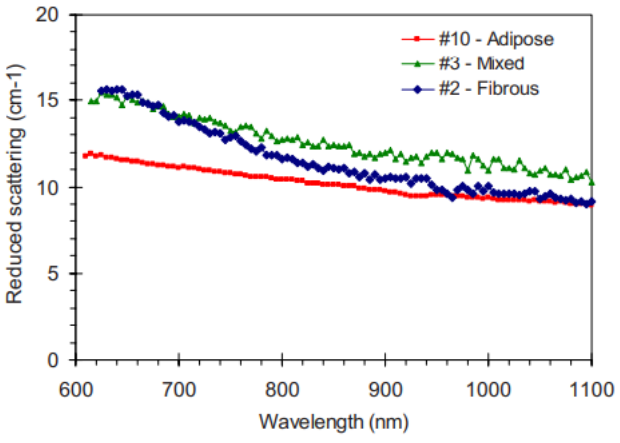

(b) Reduced scattering spectra [17].

Figure 4: Optical properties of three healthy human breast tissue in cm^{-1}, (a) absorption spectra; and (b) reduced scattering spectra. From the breasts for three healthy volunteers with different breast types. Measured using a time-resolved diffuse spectroscopy [17].

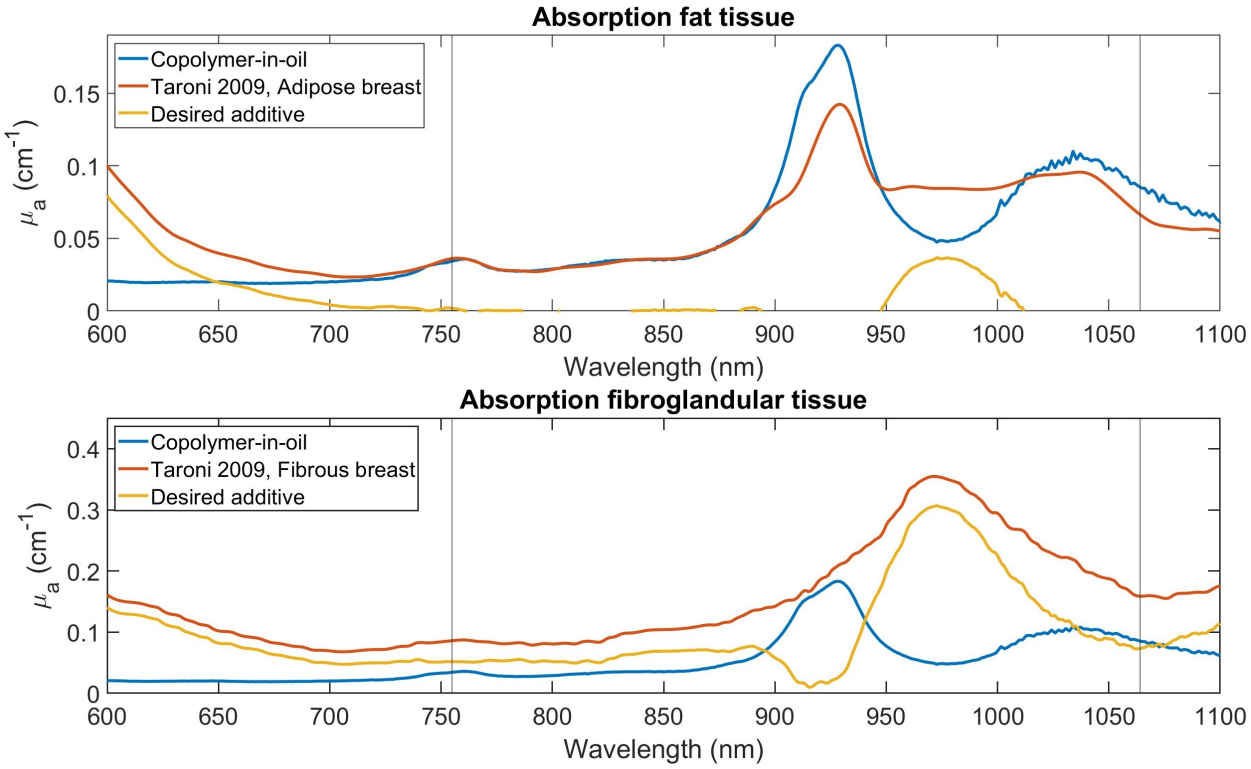

Figure 5: Absorption spectrum of the breast tissue [17] and copolymer-in-oil (the Ulm sample) [18]. The desired spectrum is obtained by subtracting the spectrum of the copolymer-in-oil from the spectrum of the literature. The two vertical lines represents the wavelength range of the PAM3.

2.3.3 Acoustic properties

The acoustic properties that need to be investigated are the speed of sound (C_s) and the acoustic attenuation coefficient (α) can be seen in Table 1. Also included in this table are the values measured by Hacker et al. for copolymer-in-oil with 12 w/w% SEBS and 4 w/w% LDPE.

Table 1: The acoustic properties of tissue in the breast.

	Speed of sound (m/s)	**Acoustic attenuation coefficient** (dB/cm/MHz)
Fatty breast tissue	1478 [19]	0.05 [20]
Fibroglandular breast tissue	1510 [19]	0.15 [20]
Copolymer-in-oil (15 w/w% SEBS, 4 w/w% LDPE)	1458 [13]	0.50 [13]

2.4 Thermoanalytical techniques

For 3D printing is it important that the temperature that is used for 3D printing is between the glass transition temperature and the melting temperature (T_g and T_m) and that it won't exceed the decomposition temperature (T_d). This will ensure the properties of the material [21]. The T_g affects the mechanical properties of the polymer. It is the temperature at which a polymer transitions from a hard, brittle or glassy state to a rubbery or viscous state. In the state above the T_g the polymer becomes more mobile [22]. The T_m is the temperature where there takes place a phase transition. Below this temperature the material is solid and above this temperature the material will be liquid [23].
These temperatures can be measured with thermogravimetric analysis and differential scanning calorimetry.

2.4.1 Thermogravimetric analysis

Thermogravimetric analysis (TGA) is a method that tracks how the weight of a material changes while it is exposed to a controlled temperature program in a controlled environment. It can be used to determine the T_d of a material. It is important to know the thermal stability of a material and up to what temperature the material is stable. In a TGA measurment a sample is heated/cooled under controlled conditions and its weight is continuously measured. It allows to observe various thermal phenomena, such as phase transitions, decomposition, and oxidation, and to determine the associated temperature ranges and kinetics [24].

2.4.2 Differential scanning calorimetry

Differential scanning calorimetry (DSC) is a technique that can be used to study the thermal properties of a material, particularly their heat capacity and thermal transitions. DSC can be used among others to determine T_m and T_g. The phase transitions can be monitored with the calorimetry. In a DSC experiment, the temperature of a sample cell and a reference cell are raised identically over time. The difference in the reference cell and sample cell would be the amount of excess heat absorbed or released by the sample [22].

3 Requirements and wishes for material and phantom

The aim is to design a breast phantom that is suitable for directly 3D printing. The requirements and wishes for the material for the phantom are shown in Table 2 and will be discussed in more detail.
The requirements and wishes were divided into two groups. The first is for the material, the second is for the final phantom. The importance factor only shows the importance within this project. Ultimately, the material and the phantom must meet all the requirements and wishes.

Table 2: The requirements and wishes for the copolymer-in-oil and for the photoacoustic breast phantom. the requirement and wishes have been scored on their importance with an importance factor from 1 to 5, with 5 the most important. Furthermore, the last column shows which requirements will be addressed within this project.

	Material/phantom	Requirement	Importance factor	This project
I	Material	Suitable for 3D printing	5	✓
II	Material	Stable and homogeneous mixture	5	✓
III	Material	Matching spectra for absorption coefficient	5	✓
IV	Material	Matching spectra for scattering coefficient	4	✓
V	Material	Matching acoustic properties	3	✓
VI	Phantom	Matching anatomy	2	
VII	Phantom	Resolution	4	
VIII	Material and phantom	Reproducible	5	

Requirement I: The copolymer-in-oil should be suitable for 3D printing. This means that the temperature used in 3D printing is between T_g and T_m of the material. The material should be able to hold the acoustic and optical properties at the temperature that is needed to print [21].

Requirement II: For the photoacoustic, thermomechanical, and longitudinal stability, of the phantom, the copolymer-in-oil should be a stable and homogeneous mixture. The optical and acoustic properties should be

the same at every point in the sample and this should remain over a certain period of time. During the process of 3D printing, the material should hold its properties.

Requirement III, IV & V: The copolymer-in-oil should have the same properties as human breast tissue given in the literature. The values and spectra of the properties can be seen in Section 2.3.2 and 2.3.3. Since the phantom is used for the PAM3, it is important that it has the same optical and acoustic properties within the same range as the PAM3 which falls at a wavelength between 720 and 860 nm [25].

Requirement VI: For characterizing and calibrating the PAM3, the phantom should look like a real human breast. The optimum case would be if the phantom cannot be distinguished from a human breast on a PA image. It should have a realistic size, shape and volume such that it fits inside the 3D printer, which has a dimension of 10 x 10 x 10 cm. The anatomy of the human breast can be seen in Section 2.3.1.

Requirement VII: The phantom design should have a minimum resolution of 750 micron, the resolution of the PAM3. The 3D printer is able to print a minimum of 200 micron.

Requirement VIII: The reproducibility is a highly important requirement since the phantom need to be used for a repeatable study. If the copolymer-in-oil is not repeatable it can not be used to characterize and calibrate the PAM3.

4 Method

In this section, the method of the experiments performed will be discussed. The details of all the materials that has been used can be seen in Appendix A.

4.1 Absorption coefficient

The main goal of these experiments is to get more knowledge in the absorption spectra of different dyes. To achieve this goal, the various dyes must be dissolved in mineral oil to obtain the spectrum of the dye in solute form. This solution measured with the spectrophotometer (SHIMADZU UV-2600). To gain an accurate spectrum, the sample needs to be homogeneous. For this reason, the samples are sonicated in an ultrasonic bath (Bransonic Z245143). The measurements with the spectrophotometer will result in the transmittance of the sample. The absorption coefficient can be calculated with the following equation's:

$$T = \frac{T(\%)}{100} = \frac{I}{I_0} \tag{3}$$

$$I = I_0 \cdot e^{-\mu_a d} \tag{4}$$

$$\begin{aligned} \mu_a &= -\frac{1}{d} \cdot \ln(\frac{I}{I_0}) \\ &= -\frac{1}{d} \cdot \ln(T) \\ &= -\frac{1}{d} \cdot \ln(\frac{T(\%)}{100}) \end{aligned} \tag{5}$$

The value obtain by the spectrophotometer is the percentage transmittance $T(\%)$. To gain the μ_a, the percentage transmittance is calculated to the transmittance T, which is the ratio of the transmitted intensity I over the incident intensity I_0. This will take a value between 0 and 1. With equation 5, μ_a can be calculated, with d in cm [26].

4.2 Copolymer-in-oil

Figure 6 and 7 and Appendix B show how the copolymer-in-oil is prepared. This involves creating the stock solution detailed in Table 3 and the copolymer-in-oil itself. The process for producing the copolymer-in-oil includes weighing all the components from Table 4, combining them, heating the mixture in an oil bath (IKA HBR 4 control), and removing any air bubbles in the vacuum oven (HERAEUS VT5042 WK, Value tool V-i120SV), as outlined in the literature [13]. This must be completed prior to pouring the copolymer-in-oil into the mold for the optical and acoustic characterisation. For the quantities of SEBS, LDPE, and mineral oil required to attain the desired acoustic and optical properties for a breast phantom, see Tables 3 and 4. For the stock solution to become homogeneous, it is necessary to heat the mineral oil and wax and sonication in an ultrasonic bath (Bransonic Z245143).

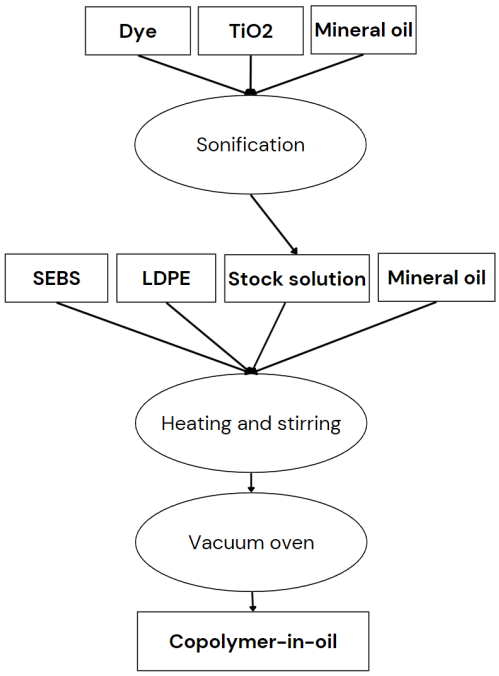

Figure 6: Flow scheme for production copolymer-in-oil, based on protocol of Hacker et al. [13].

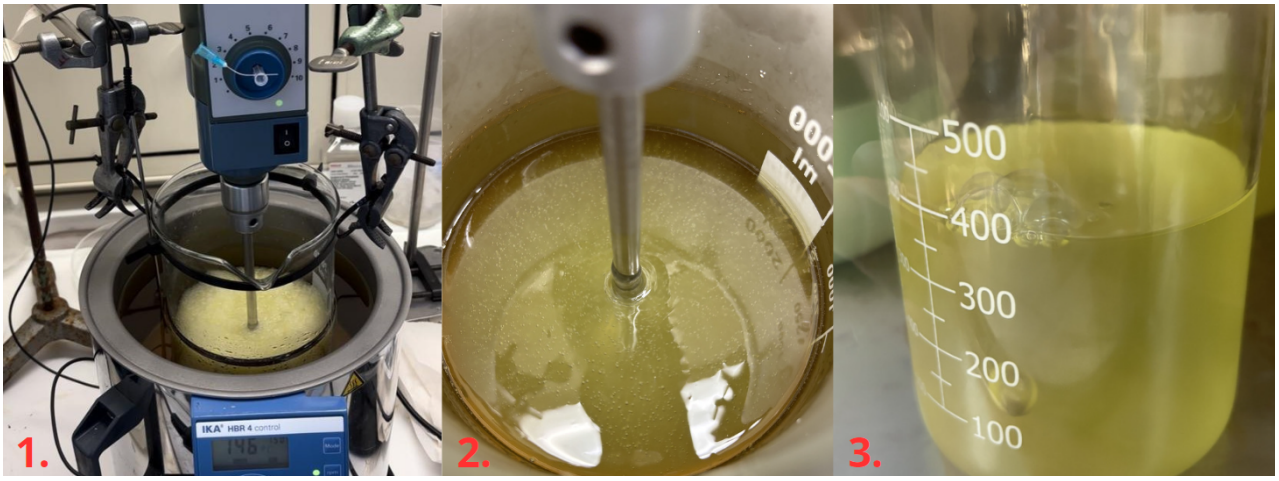

Figure 7: Pictures of the process of making the copolymer-in-oil. 1. The setup of the 'heating and stirring'; 2. The mineral oil with SEBS, LDPE and part of the stock solution after about an hour in the oil bath; 3. The copolymer-in-oil in the vaccuum oven.

Table 3: The components for the stock solution to get 3.03 w/w% yellow wax, 96.97 w/w% mineral oil.

	w/w%	Volume (ml)	Amount (g)
Mineral oil	96.97	40	33.22
Yellow wax	3.03		1.038
Total	100		34.248

Table 4: The components for the copolymer-in-oil to get 12 w/w% SEBS, 5 w/w% LDPE, 0.03 w/w% yellow wax.

	w/w%	Volume (ml)	Amount (g)
Mineral oil	82	750	624.750
SEBS	12		91.427
LDPE	5		38.095
Stock solution	1		7.61
Total	100		761.890

4.3 Characterisation of the copolymer-in-oil

The optical and acoustic properties of the copolymer-in-oil must be determined. This section focuses on the method for characterising these properties.

4.3.1 Optical properties

For the characterisation of the optical properties of the copolymer-in-oil, the same method can be used as described in Section 4.1. The sample can be measured with the spectrophotometer. The measurements with the spectrophotometer will result in the transmittance of the sample. With equation 5 the μ_a can be calculated. With d the thickness of the sample and $T(\%)$ the obtained transmission. The μ_a can be plotted against the wavelength (nm).

4.3.2 Acoustic properties

The speed of sound and the acoustic attenuation can be derived with the setup shown in Figure 9, a more detailed picture of the set up for the transducer, the sample and hydrophone needle can be seen in Figure 8. It consist of an US transducer (Panametrics v303, v306 or v309), a hydrophone needle (Precision acoustics SN 1887), a pulse-receiver (Panametrics 5077PR), a oscilloscope (Tektronix TDS 2024C and Picoscope 2204A) and a water bath. The sound wave, which is produced with the pulse receiver and the US transducer, propagates through the water and through the sample. The signal is then detected by the hydrophone needle and processed by an oscilloscope on the computer.
The entire protocol for obtaining the acoustic properties can be seen in Appendix E.

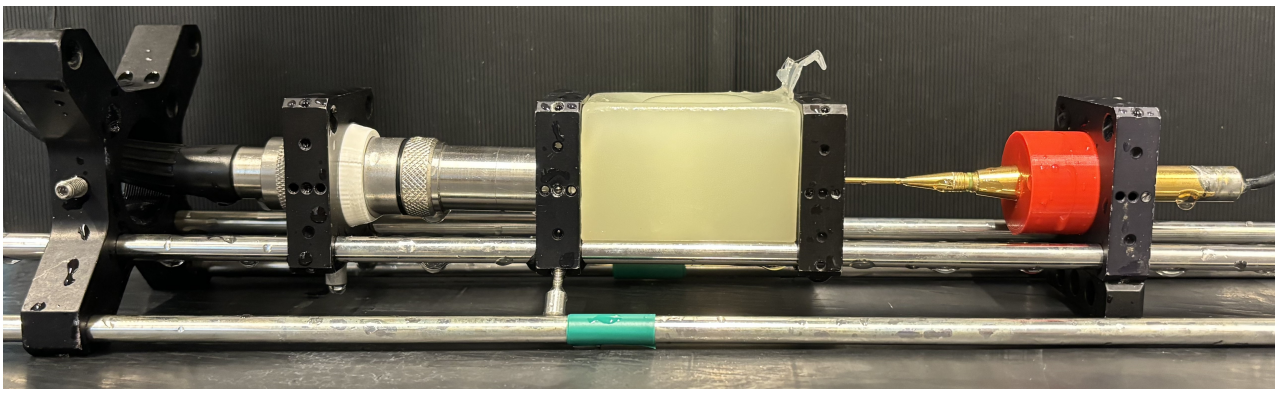

Figure 8: A picture of the set up for the measurements for the acoustic properties. It is zoomed in on the part that will be in the water bath. From left to right, the transducer, the sample and the hydrophone needle.

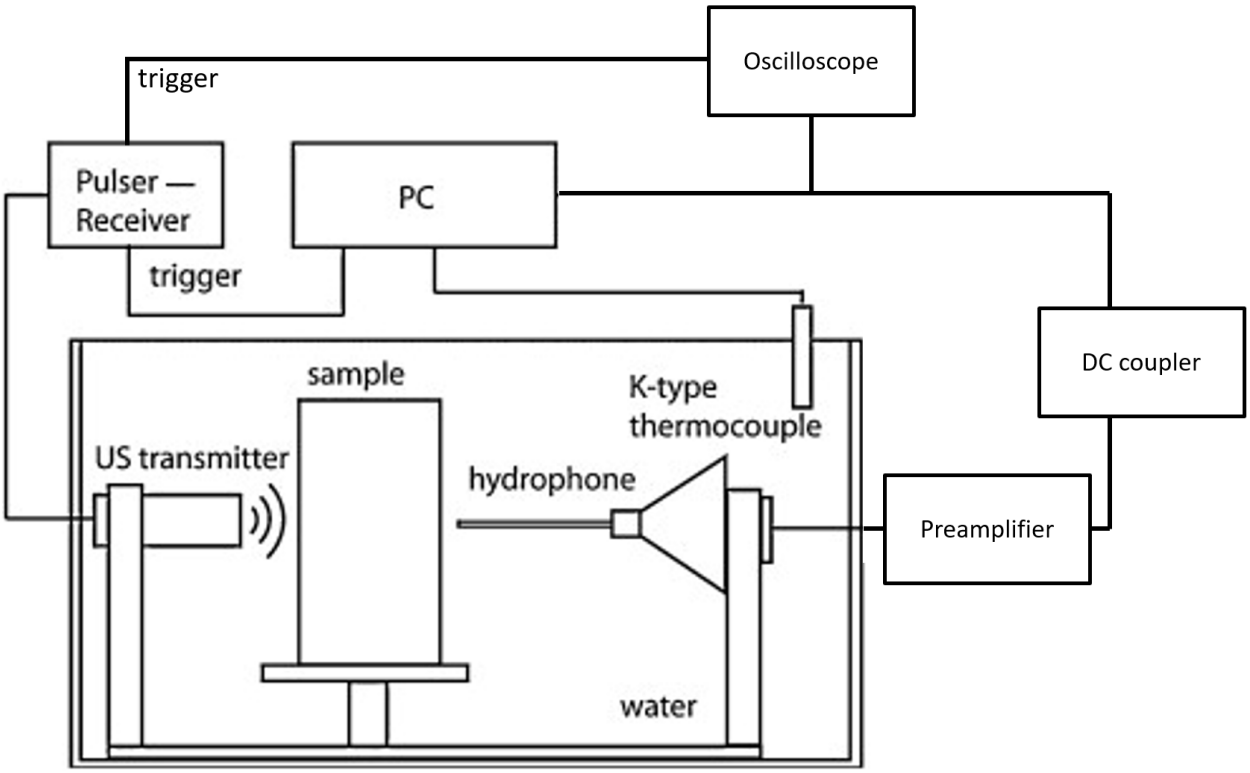

Figure 9: A schematic overview of the used set up for measuring the speed of sound and the acoustic attenuation with an US transducer, Pulser-receiver, oscilloscope and hydrophone needle. [27].

Speed of sound

To obtain the wave from two known thicknesses to derive Δt, the speed of sound measurements should be performed twice with the second time the sample turned a quarter turn. The speed of sound of the sample (C_s) can then be calculated with the following equation:

$$C_s = \frac{\Delta d}{\Delta t + \frac{\Delta d}{C_w}} \tag{6}$$

The derivation of this equation can be seen in Appendix C. With the difference in thickness, Δd, of the sample, with $d_{thin} - d_{thick}$. The difference in time, Δt, at which the US wave reaches the hydrophone needle, with $t_{thin} - t_{thick}$. And the speed of sound of the water at a specific temperature is C_w. Two methods to derive the Δt can be used. The first method is to compare the times of the peaks. The second method is to compare the times of the first point where the wave passes a certain threshold.

When C_s is greater than C_w, the time signal when propagating through the thick side of the sample block will arrive earlier than when measured through the thin side of the sample block. As a result, Δ t is negative.

The attenuation coefficient is determined by three different transducers, this is sufficient to measure the speed of sound in triplo.

Acoustic attenuation coefficient

The measurements of the acoustic attenuation coefficient should be done with three different transducers; 1, 2.25 and 5 MHz. This is because the acoustic attenuation coefficient is dependent on the frequency. The amplitude of the sound waves should be compared with travelling through the thick and thin side of the sample. The acoustic attenuation is determined by how much of the signal has dissipated over the sample thickness. The equation by which acoustic attenuation can be calculated is:

$$\alpha_s(\omega) = \frac{20}{\Delta d}\log(A_\omega) = \frac{20}{\Delta d}\log(\frac{A_{thin}(\omega)}{A_{thick}(\omega)}) \tag{7}$$

In this equation, A_ω is the amplitude-ratio of the sound waves when travelling through the two different thicknesses of the sample. The attenuation coefficient of the sample is given with $\alpha_s(\omega)$ in dB/cm. Since the

acoustic attenuation coefficient (dB/cm/MHz) is dependent on the frequency, the three different transducers are used [27].

Density
The density of the copolymer can be calculated with the following equation:

$$\rho = \frac{m}{V} \tag{8}$$

In this equation ρ is the density in g/L, m is the mass in g and V is the volume in L.
The mass of the sample can be weighted on a scale. And the volume of the sample can be determined by immersing it in water and measuring the amount of water displaced. This is according to Archimedes' law: an object displaces a volume of liquid equal to its own volume [28].

The acoustic impedance
The acoustic impedance of the sample can be calculated with the following equation:

$$Z = \rho \cdot C_s \tag{9}$$

C_s is the speed of sound of the material and ρ is the density [27].

4.3.3 Thermal analysis

To better understand whether the material is potentially suitable for 3D printing, thermoanalytical measurements need to be conducted. Two types of techniques will be discussed. The work was performed in a collaboration and by members of the Engineering Organ Support Technologies at the University of Twente (contact: V. Trikalitis -MSc).

Thermogravimetric analysis
A TGA is comprised of a sample pan positioned on a precise balance within a furnace, which is then heated or cooled as the experiment progresses. The analyzer continuously tracks the sample's mass throughout the procedure. The weight (%) will be plotted against the temperature (°C).

Differential scanning calorimetry
In a DSC experiment, the temperature of a sample cell and a reference cell are raised identically over time. The difference in the reference cell and sample cell would be the amount of excess heat absorbed or released by the sample [22]. The DSC (μV/mg) will be plotted against the temperature (°C).

5 Results

5.1 Absorption coefficient

Different dyes have been tested for absorption coefficient to better match the spectra of the absorption coefficient of the breast tissue [17]. This was done by dissolving the dyes in mineral oil and measuring the transmission. With equation 5, the absorption coefficient can be calculated for every wavelength. From this, the spectra were obtained that can be seen in Figure 10.

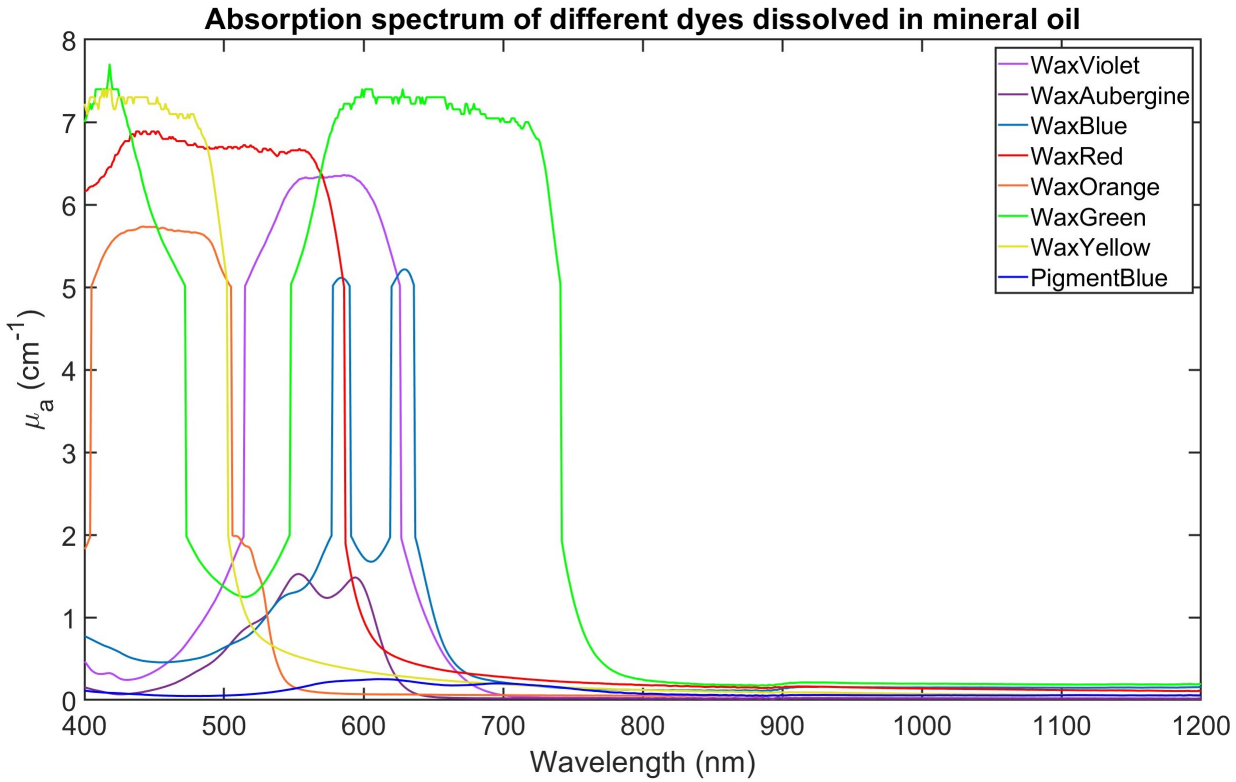

Figure 10: The absorption coefficient of different dyes

The yellow and red waxes have been tested further because they have shown potential in Figure 10 in mimicking the absorption spectrum of the breast from Taroni et al. [17]. Two different concentrations of the waxes dissolved in mineral oil were tested. This can be seen in Figure 11.

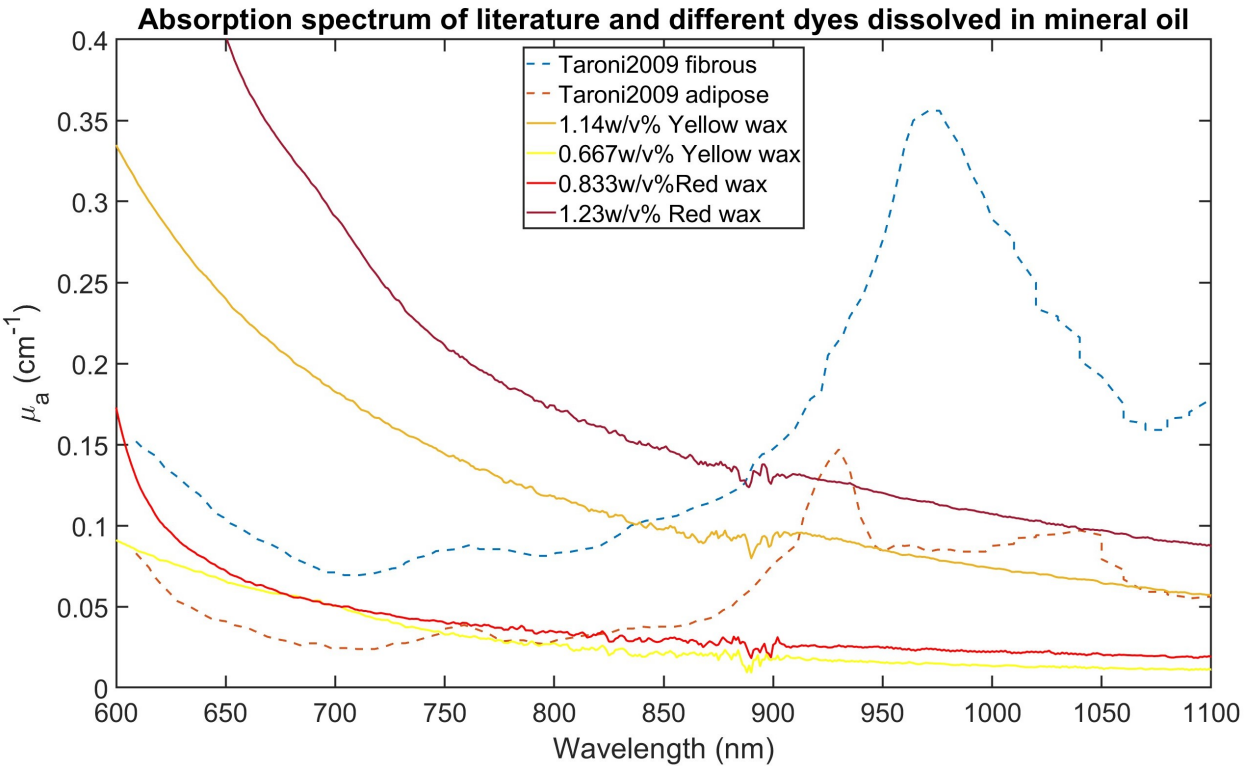

Figure 11: The absorption coefficient of different dyes compared to the spectra from the literature [17].

5.2 Copolymer-in-oil

The whole protocol of making the copolymer-in-oil can be seen in Appendix B. The steps of the process are summarized with pictures taken during the process in Figure 12.

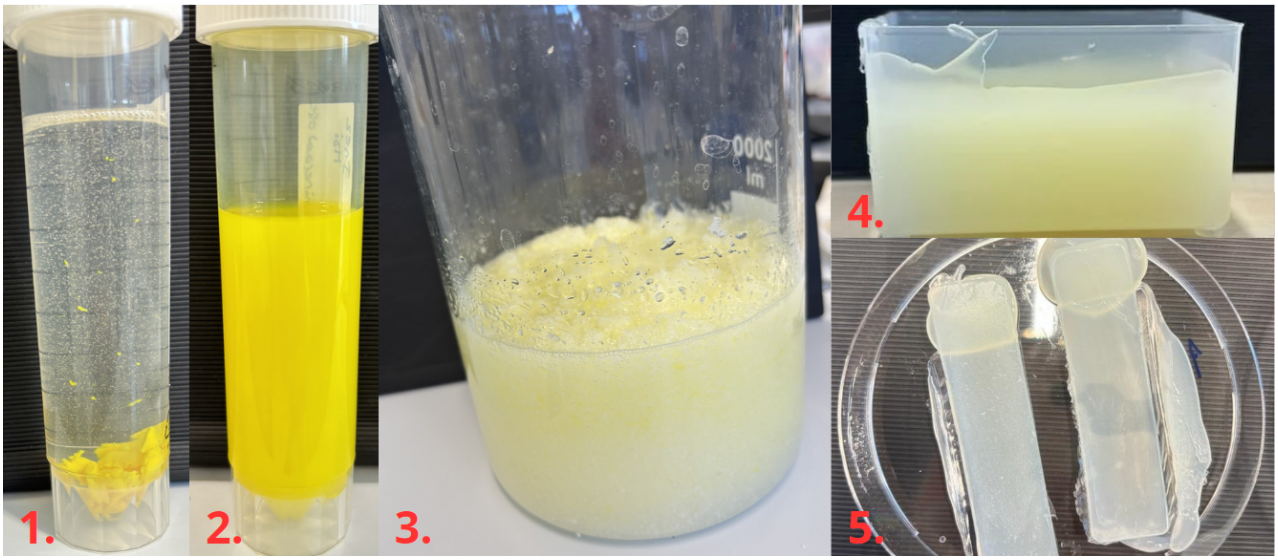

Figure 12: Pictures of the process of making the copolymer-in-oil. 1. The stock solution with mineral oil and yellow wax before the sonication; 2. The stock solution after the sonication; 3. The mineral oil with SEBS, LDPE and part of the stock solution before entering the oil bath; 4. The copolymer-in-oil in the acoustic mold; 5. The copolymer-in-oil in the optical mold.

As can be seen in the figure, the copolymer-in-oil will is poured in two types of molds. The first one is for the acoustic measurements. Only one block has been made for the acoustic characterisation.
The second type of mold is for the optical measurements. For the optical characterisation four different samples have been made. These are called A1, A2, B1 and B2.

5.3 Characterisation of the copolymer-in-oil

5.3.1 Optical characterization

The obtained data from the spectrophotometer is processed with the Matlab script from Appendix D. The script is based on equation 5. The obtained figure of the Matlab script is shown in Figure 13. The black line is from the copolymer-in-oil that has been made and the blue and red lines are the spectra of Taroni et al. [17].
Sample A1 was used for both methods which has a thickness of 3.13 mm. The sample consists of 12 w/w% SEBS, 5 w/w% LDPE, 0.03 w/w% yellow wax and 82.97 w/w% mineral oil. The values of SEBS and LDPE are based on the protocol of Hacker et al. [13] and the concentration of yellow wax is based on Section 5.1. The protocol for making the sample can be seen in Appendix B.

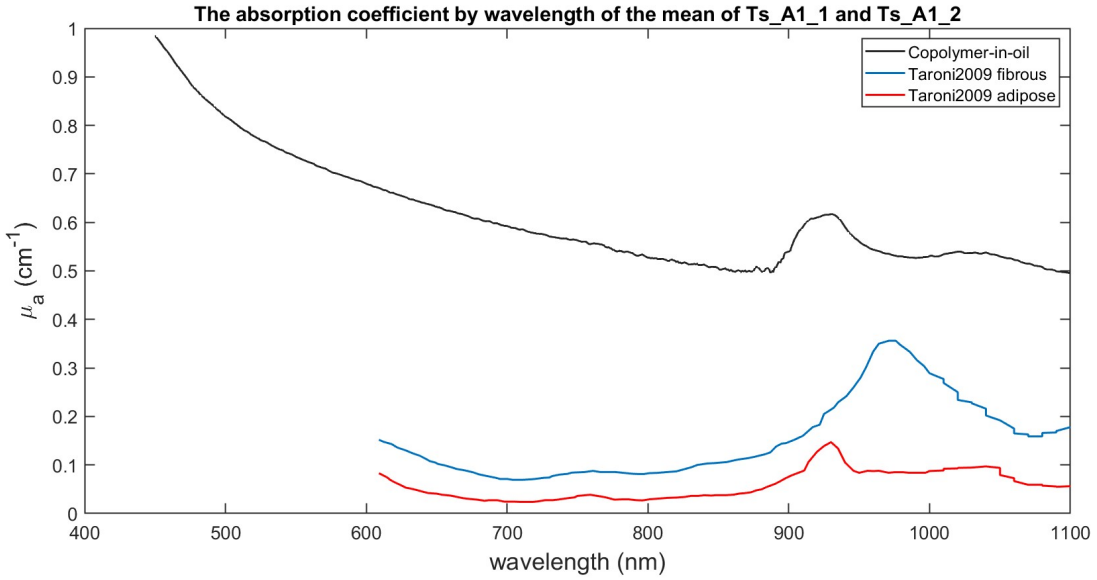

Figure 13: The obtained spectrum of the absorption coefficient of the copolymer-in-oil. The spectrum was obtained using the method described in Section 4.1 [17].

5.3.2 Acoustic characterization

The obtained US signals are plotted in Figure 14, 15, 16 and 17, using the Matlab script in Appendix G. In the Matlab script, the speed of sound of water is generated using the Matlab function in Appendix G. The temperature of the water during the measurements was 22.8 °C.

Speed of sound

In Figure 14, the US signals over time the test block is given measured with three different frequency transducers. The test block is copolymer-in-oil, with 82.97 w/w% mineral oil, 12 w/w% SEBS, 5 w/w% LDPE and 0.03 w/w% yellow wax (Rayher).

It can be seen that, when measured through the thin side (full line), the US signal reaches the hydrophone later than when measured through the thick side (dashed line).

The obtained speed of sound of the copolymer in oil are shown in Table 5, which shows the two different methods of determining Δt with the three different transducers. The overall mean of the six values is 1531.92 m/s. The differences in results that the two methods gave, and which method is most accurate, will be explained in the discussion, Section 6.

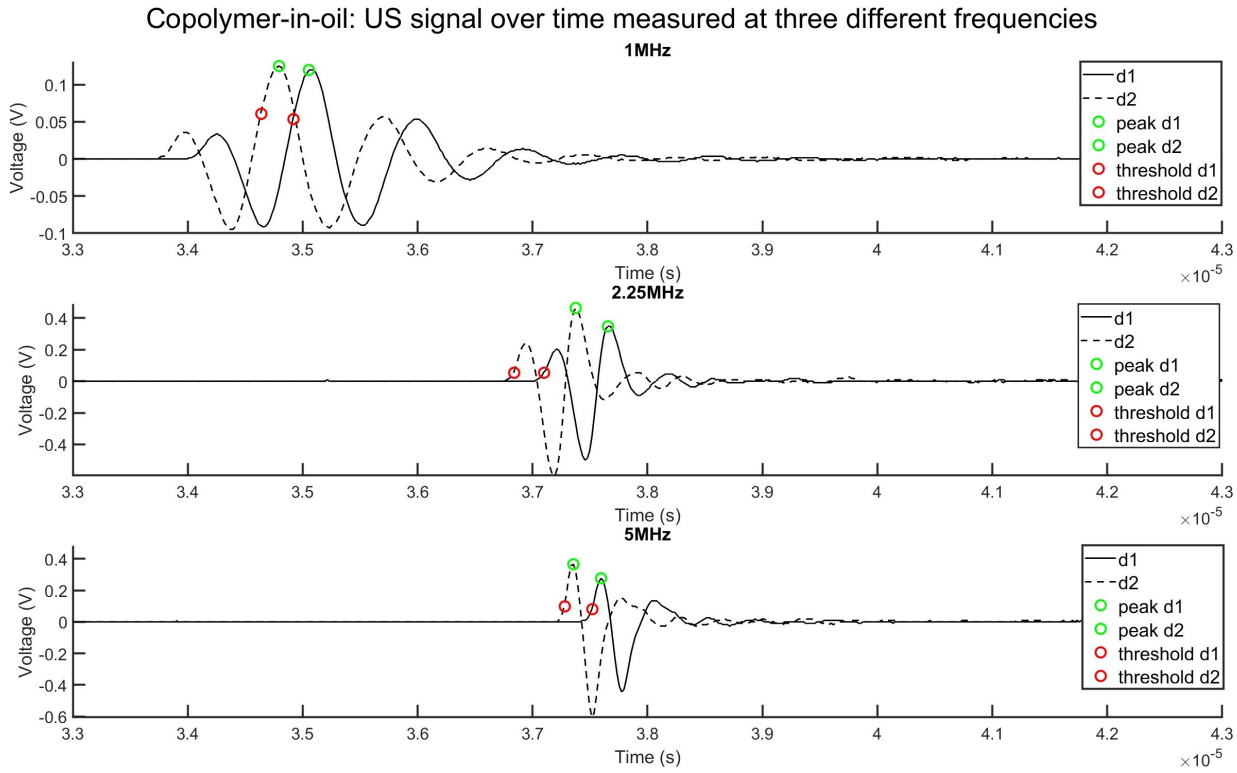

Figure 14: US signal over time of a block of copolymer-in-oil measured with a hydrophone needle with three different transducer frequencies (1.00, 2.25 and 5.00 MHZ). Two different measurement thicknesses (thin and thick, d1 and d2 respectively) were created by turning the rectangular block a quarter turn. This block consists of copolymer-in-oil obtained by following the protocol in Appendix B.

Acoustic attenuation

The acoustic attenuation was obtained by two different methods. Taking the amplitude difference of the highest peaks and putting these values in equation 7 is the first method. The second method entails choosing the frequency region from Figure 15, approximately defined by the full width at half maximum (FWHM), and then computing the attenuation coefficient across this frequency range. This approach generates graphs displaying how the values change over a range of frequencies instead of representing single values associated with a peak. Here, for each frequency, a line was obtained. See Figure 16. The 'Curve Fitter Tool' from Matlab was used to perform polynomial fitting across these three lines. This can be seen in Figure 17.

In Table 5 can the attenuation coefficient of derived from the two different methods been seen. The values for the attenuation coefficient determined from the polynominal fit are much higher than the ones determined from the highest peaks. The differences in results that the two methods gave, and which method is most accurate, will be explained in Section 6.

Table 5: The speed of sounds and attenuation coefficients iwth different transducers of the copolymer-in-oil obtained by following the protocol in Appendix B.

Measuring frequency (MHz)	Speed of sound from highest peak (m/s)	Speed of sound from threshold (m/s)	Attenuation coefficient from highest peaks (dB/cm)	Attenuation coefficient from polynomial fits (dB/cm)
1	1531.91	1535.17	0.264	1.3757
2.25	1535.17	1531.91	1.732	1.9781
5	1528.67	1528.67	1.683	3.3033

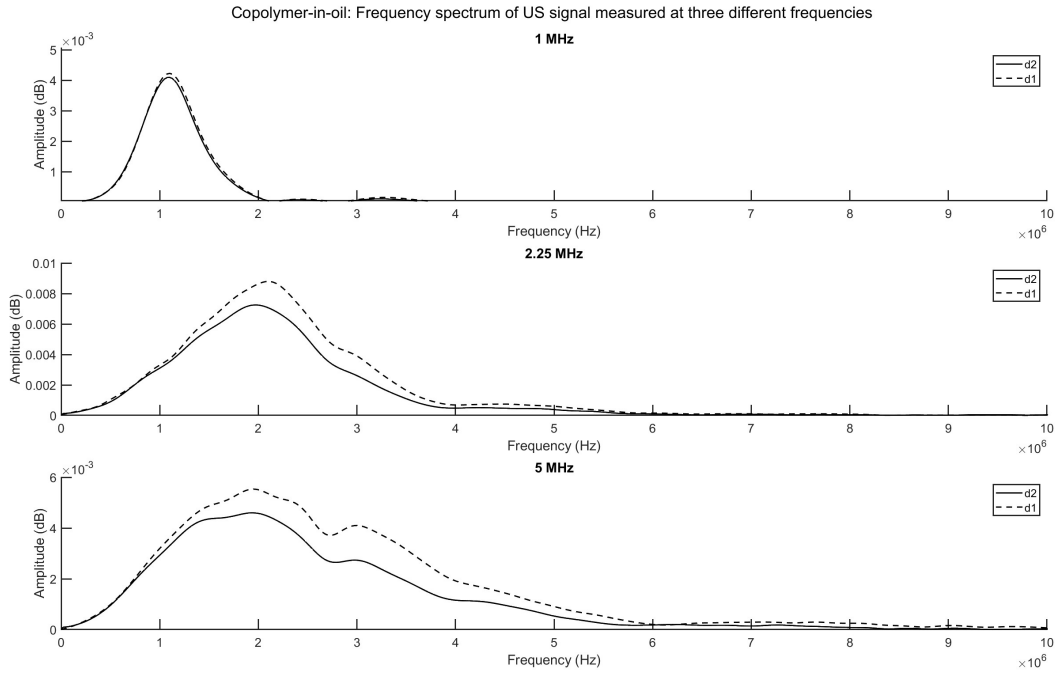

Figure 15: Frequency spectra of a block of copolymer-in-oil measured with a hydrophone needle at three different transducer frequencies (1, 2.25 and 5 MHz). Two different measurement thicknesses (thin and thick, d1 and d2 respectively) were created by turning the rectangular block a quarter turn. This block consists of copolymer-in-oil obtained by following the protocol in Appendix B.

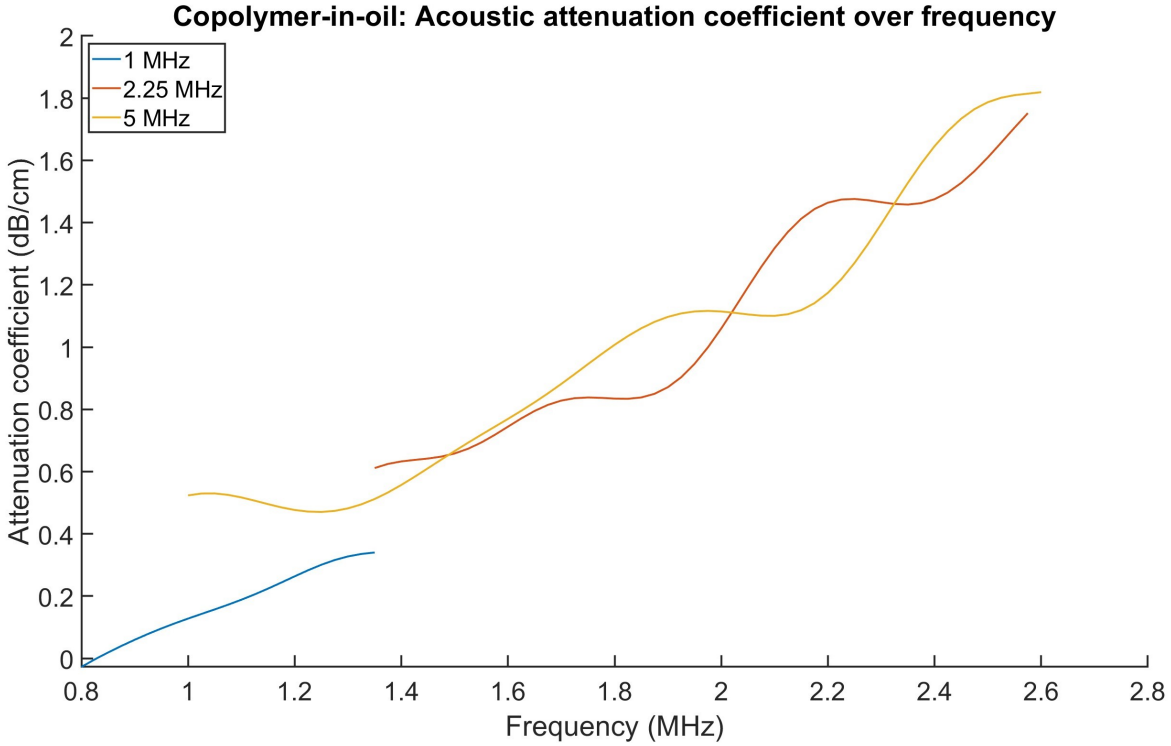

Figure 16: Acoustic attenuation coefficients of the block of copolymer-in-oil over frequency. for each measuring frequency (1, 2.25 and 5 MHz), a frequency region was selected (FWHM) to calculate this coefficient. This block consists of copolymer-in-oil obtained by following the protocol in Appendix B.

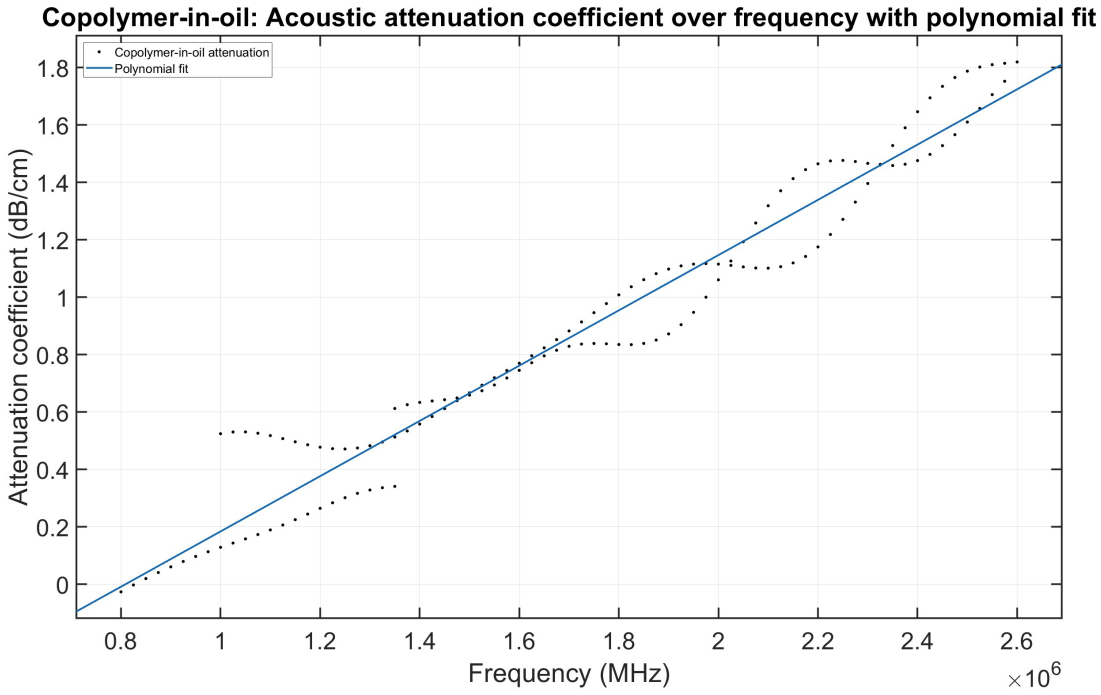

Figure 17: Acoustic attenuation coefficients of the block of copolymer-in-oil over frequency. For each measuring frequency (1, 2.25 and 5 MHz), a frequency region was selected (FWHM) to calculate this coefficient. The polynomial fit through these curves is also given in blue. The fit has a equation of $\alpha = 0.4819f + 0.8938$. This block consists of copolymer-in-oil obtained by following the protocol in Appendix B.

Density

The density of the test block was calculated with equation 8. In this equation the mass of the block is divided by the volume to derive the density. The values of the mass and the volume can be seen in Table 6.

Table 6: The values of the volume, mass and density of the copolymer-in-oil. This block consists of copolymer-in-oil obtained by following the protocol in Appendix B.

Volume (L)	Mass (g)	Density (g/L)
0.055	46.54	846.2

The acoustic impedance

The acoustic impedance of the test block was calculated with equation 9 where the density is multiplied by the speed of sound to obtain the acoustic impedance. The speed of sound that has been used is the mean speed of sound of the six values, 1531.92 m/s.

Table 7: The values of the density, speed of sound and the acoustic impedance of the copolymer-in-oil. This block consists of copolymer-in-oil obtained by following the protocol in Appendix B.

Density (g/L)	Speed of sound (m/s)	Acoustic impedance (MRayl)
846.2	1531.92	1.30

5.3.3 Thermal analysis [1]

Thermogravimetric analysis

In Figure 18 starts the graph at a weight of 100 %. This means that the weight of the sample is the complete weight when compared to the beginning of the experiment. At around 140 °C the weight starts to decrease as the graph descends. The reason of this descend will be discussed in Section 6.

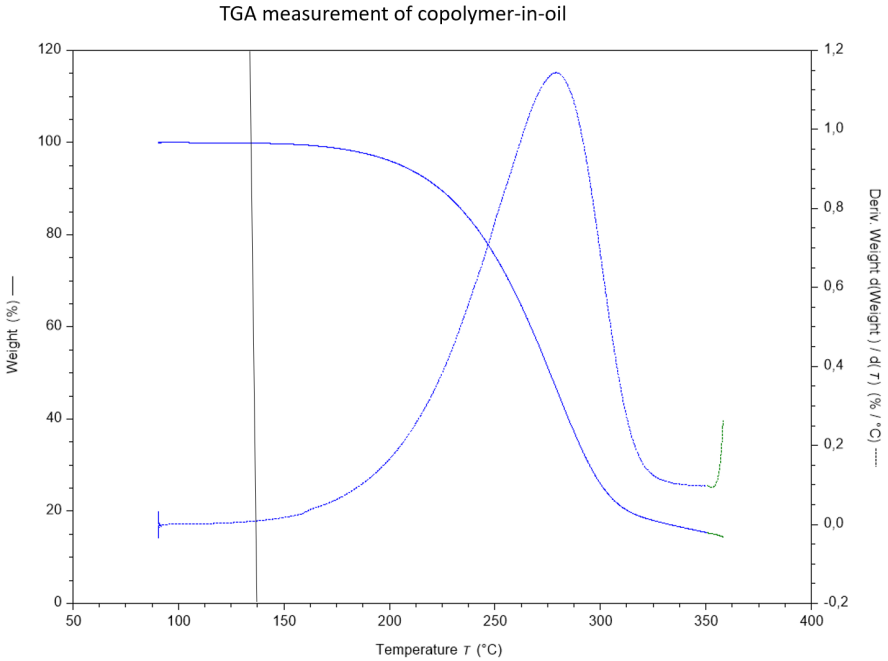

Figure 18: The TGA measurement of the copolymer-in-oil obtained by following the protocol in Appendix B.

Differential scanning calorimetry

In Figure 19 can the heat flow be seen for different temperatures. At around 78 °C starts the graph to descends, at around 90 °C there is a peak and it will increase until around 100 °C. Furthermore, at 45 °C the curve starts to flatten. The reason of this peak will be discussed in Section 6.

[1] These experiments and data processing are conducted by V. Trikalitis (MSc.) from the Engineering Organ Support Technologies at the University of Twente

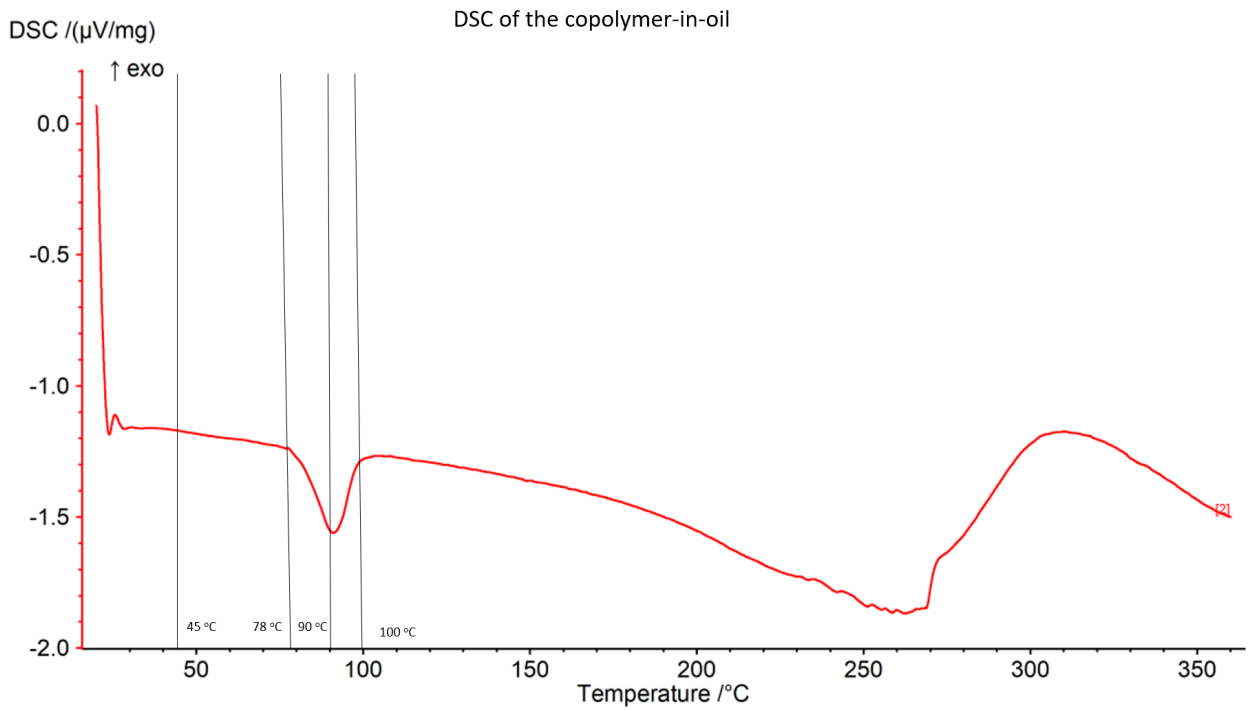

Figure 19: The DSC measurement of the copolymer-in-oil obtained by following the protocol in Appendix B.

6 Discussion

6.1 Absorption coefficient

A dye can be used to optimize the μ_a of the material. To gain a better understanding of the absorption spectrum of different dyes, they were dissolved in mineral oil and then measured by a spectrophotometer.

In Figure 10 the absorption coefficient spectra from different dyes can be seen. The spectrum should be the same as the desired additive from Figure 5. The desired additive spectrum is the spectrum of breast tissue from which the spectrum of copolymer-in-oil with the base concentrations has been subtracted. This means that a substance must be added which ultimately has the desired additive spectrum as its spectrum.
The violet and aubergine wax both have an excessively steep spectrum of 600 to 700 nm. This makes it unsuitable for copolymer-in-oil for fatty and fibroglandular tissue. The blue wax shows a good slope after 700 nm, but this should have been at a lower wavelength. The orange wax has too early a peak, which also makes it unsuitable as a dye. The green wax has a broad peak that is not desirable from about 600 nm onwards. The yellow and red wax, from Rayher, show good potential for the dye. So, these have been tested further.
In Figure 11 the spectra of the yellow and red wax with different concentrations are shown. From this figure can be concluded that the yellow wax has the most potential. This can be explained because female breast tissue also has a yellow color. The exact concentration of the yellow wax must be changed to match the height of the graph.

6.2 Copolymer-in-oil

In making the copolymer-in-oil according to Hacker et al. the stock solution is sonicated in a bath with a temperature of 90 °C [13]. The sonicator bath used here has a maximum temperature of 69 °C. The bath has difficulty with rapid heating. Therefore, there was water removed from the bath and replaced with hot water from the tap [29].
To get a clean material, it is important to get all the material from the same bottle. But when weighing the SEBS and mineral oil, there was not enough material in both. Therefore, two different bottles were used.
In the protocol of Hacker et al. [13] the oil bath uses a magnetic stirring bar . This did not have enough power

for the quantity now made. Therefore, it was chosen to stir it with a mechanical stirrer. The magnetic stirring bar was turned on, in order to heat the oil bath homogeneously, at 150 rpm.
The protocol of Hacker et al. [13] says that the mold can be oiled with an oil other than mineral oil. To remove the optical samples from the plastic storage box, the non-adhesive spray (Trennspray Voss loswas 400gr) used for the molds was not enough. Therefore, it was chosen to oil the plastic container with mineral oil anyway.

6.3 Characterisation of the copolymer-in-oil

6.3.1 Optical characterization

In Figure 13, a complete spectrum of μ_a is shown. Notably, this graph exhibits high values from 450 to 800 nm. This can be explained by the yellow wax. The expectation was it to be around 0.1 cm^{-1}, not at 0.98 cm^{-1}.
In addition, the graph is about six times higher than the values of the breast tissue of Taroni et al. [17]. The reason for this difference is that the material scatters the light a bit. The scattered light arrives at the detector. This seems like there is transmission of the light, so the transmission and absorption coefficient will be higher. Given the notably higher values, it is hard to say something about the suitability of the absorption coefficient of copolymer-in-oil as a breast tissue mimicking material.

When measured, the samples were removed from the plastic container in which it is kept. When the sample was taken out, a thin layer was left in the plastic. A photograph of this can be seen in Appendix C. This makes it uncertain whether the sample has a smooth surface. And if it does not, it is not known what impact it would have.

6.3.2 Acoustic characterization

To obtain a proper signal, the best settings were considered for each transducer. Thereby, the pulser voltage at the 5 MHz transducer was not 100 but 400 V. This has no influence on the final obtained speed of sound and acoustic attenuation because a comparison is made between the two measurements of the same transducer.

In Figure 14, notice that the wave from the thin side arrives earlier than the wave from the thick side. This is because the speed of sound of the copolymer-in-oil is lower than the speed of sound of water, causing the following effect. The longer the US waves have to travel through the sample, the longer the path with a lower speed of sound. Resulting in the US waves propagating through the thick side of the block arriving at the hydrophone needle at a later point in time.

As can be seen from the results from the speed of sound characterization, Table 5, the mean speed of sound of the two methods and each three transducer is 1531.92 m/s. The speed of sound of the literature can be seen in Table 1. It is important that the speed of sound of the copolymer-in-oil is the same as that of breast tissue so that a realistic PA breast phantom can be made with it. As can be seen from these values is that the speed of sound of the copolymer-in-oil that has been made is higher than the desired speed of sound for the fatty and fibroglandular tissue. The speed of sound can be decreased by changing the concentration of LDPE. According to Hacker et al. [13] the concentration of LDPE has a linear concentration with the speed of sound. By increasing the concentration, the speed of sound will also increase. For this reason, the LDPE concentration should be decreased to match the speed of sound of the fatty and fibroglandular tissue. But further research should be done to know the exact concentration.
The speed of sound is measured with two different methods. The first method is from every wave the highest peak and the second method is from every wave the first time the wave passes a certain threshold. The two methods should give basically the same speed of sound, because the speed of sound is based the difference in time between the two waves as long as the same point is chosen for each wave. Whether it is a certain threshold or whether it is the highest point should not matter. However, for the 1 and 2.25 MHz transducer, the results are different. It is noticeable that the average of the two methods are exactly the same. This is because both methods contain the same values, but for other frequencies. Because of the same average, it is not possible to say which method is the best method to determine the speed of sound.

The acoustic attenuation coefficient was determined in two ways, as described in Section 5.3.2. The values can be seen in Table 5. When determining the attenuation coefficient with the highest peak, the coefficient is lower than determining it with the polynomial fit.
Figure 15 shows that at the 1 MHz transducer, the difference in the two peaks is minimal. The difference between the "thick" and "thin" measurements over a certain range was also considered and a trend line was extracted by using the polynomial fit, this can be seen in Figure 17. Here, the FWHM value was chosen. This should give a more accurate value because it is averaged over a range of frequencies. It is not reflected in the results that this way becomes more accurate. The reason is that not every graph in Figure 15 has the same shape, whereas it should have the same shape. But overall is the method for deriving the attenuation coefficient from the polynomial fit better than the of the highest peaks. This is because the attenuation coefficient has a linear fit with the frequency. This is not the case for the highest peak, but it is for the polynomial fit.
In addition, in Figure 15 the frequency value peak of the transducer should fall on the transducer used. So, the peak of the 1MHz transducer, should be seen at a frequency section of 1MHz. For the 2.25 and 5 MHz transducer at a frequency of 2.25 and 5 MHz, respectively. This is approximately the case with the 1 and 2.25 MHz transducer, but not with the 5 MHz transducer. The reason for this can probably impairments in the transducer or in the hydrophone needle. In further research, testing can be done with another 5 MHz transducer and/or another 1mm hydrophone needle.

6.3.3 Thermal analysis

From Figure 18 can be seen that the weight of the sample started to decrease at around 140 °C. This means that the decomposition of the copolymer-in-oil occurs at around 140 °C. This means that the material is thermally stable up to this temperature. After that, it starts to degrade.
In Figure 19, everything beyond 140 °C can be disregarded due to the process of decomposition. At the starting temperature the copolymer-in-oil still retain its native shape and structure. As the sample heat up, the material begins to thermally denature. This can be seen at around 78 °C. The heat flux increases as the material unfolds. The T_m is the point where 50% of the material is native and 50 % is denatured, this is at 90 °C. The melting transition has completed at 100 °C and the material behaves the same as before in terms of heat flux, but now its liquid instead of solid which does not affect heat flux. The flattening of the curve at 45 °C represents the T_g of SEBS.
By this information, it can be said that the copolymer-in-oil is potentially suitable for 3D printing. In fact, the temperature used in 3D printing is between melting point and glass transition temperature.

7 Conclusion and Outlook

The objective of this study was to explore methods for improving the recipe of copolymer-in-oil phantom material to better match the optical and acoustic properties of breast tissue, with a focus on fatty and fibroglandular tissue, in order to create a more realistic and accurate breast tissue-mimicking material suitable for 3D bio-printing.
Through the use of various dyes dissolved in mineral oil, it was determined that the yellow wax showed the most potential for replicating the absorption coefficient (μ_a) of breast tissue, as it matched the tissue's color and exhibited suitable absorption characteristics. The exact concentration of yellow wax needs further adjustment to align with breast tissue properties.
In general, the protocol of Hacker et al. [13] is a good method for making copolymer-in-oil. In which the acoustic and optical properties can be well tuned. Some practical challenges were encountered in the copolymer-in-oil preparation process. The temperature of the sonication bath and issues with heating were observed, indicating the need for better temperature control.
Optical characterization revealed that the actual μ_a spectrum of the material significantly deviated from the target, particularly in the 450 to 800 nm range. This discrepancy can be attributed to the yellow wax used. Moreover, the graph indicates values roughly six times higher than those of natural breast tissue, possibly due to scattering effects. The scattering might reach the detector's front surface, mimicking higher transmission.

The speed of sound in the copolymer-in-oil was found to be higher than the desired values for fatty and fibroglandular tissue, namely 1531.92 m/s. LDPE concentration adjustments are required to match the material's speed of sound with that of breast tissue.
The thermal analysis shows that T_g is at 45 °C, T_m at 90 °C and T_d at 140 °C With this information it could be said that the material is potentially suitable for 3D printing.

In conclusion to the research question "*How can the recipe of copolymer-in-oil phantom material be improved to match the optical and acoustic properties of breast tissue, specifically fatty and fibroglandular tissue, to create a more realistic and accurate breast tissue-mimicking material that is potentially suitable for 3D printing?*" further refinements to the copolymer-in-oil recipe are necessary. These adjustments should address both the optical properties, particularly μ_a matching through yellow wax concentration modification, and the acoustic properties, focusing on fine-tuning the LDPE concentration to align with the speed of sound in breast tissue. With current concentrations, copolymer-in-oil is potentially suitable for 3D printing.

This research lays the groundwork for improving copolymer-in-oil as a phantom material for photoacoustic and ultrasound breast imaging, potentially advancing the field of medical imaging and diagnostics.

7.1 Oulook

Future research should focus on fine-tuning the recipe of copolymer-in-oil to more accurately match the optical properties of breast tissue, especially the absorption coefficient (μ_a). Continued experimentation with the concentration of yellow wax and other suitable dyes may lead to a closer resemblance to natural tissue. It should also focus on the method for obtaining the μ_a and $\mu_s^{'}$.

With the material demonstrating potential suitability for 3D printing, future work should explore its application in creating realistic breast phantoms for advanced 3D printing techniques. So a detailed breast mimicking phantoms can be printed.

Subsequent research should involve validating the improved copolymer-in-oil phantoms in a clinical context. Assessing their performance in photoacoustic and ultrasound breast imaging will be crucial for translating this work into practical medical applications.
Collaborative efforts involving experts in materials science, medical imaging, and breast cancer research can further advance the development and application of these realistic breast phantoms. Interdisciplinary research will be key to achieving meaningful breakthroughs.
In summary, the journey to creating an ideal breast tissue-mimicking material for 3D bio-printing is ongoing. The insights gained from this study set the stage for more refined materials that can significantly enhance the field of medical imaging and diagnostics, particularly in the context of breast cancer detection and research. The road ahead is filled with opportunities to create more accurate phantoms that can contribute to improved patient care and medical innovation.

8 Acknowledgement

First of all, I would like to thank Prof. Dr. Srirang Manohar for giving me the opportunity to do my bachelor assignment in the research group of Multi-Modality Medical Imaging. Without his extensive feedback and guidance, I would not have been able to write this thesis. Thank you for the daily guidance and for encouraging me to the always get the best out of myself. Also a special thanks to my daily supervisor Ir. Rianne Bulthuis for always answering my questions, helping me with experiments and clear feedback. I would also like to thank Dr. ir. David Thompson , Prof. Dr. Srirang Manohar, Ir. Rianne Bulthuis for wanting and making the time to be a part of the committee.

I would like to express my gratitude to all members of the M3I photoacoustic research group for our weekly meetings. Your insights have been invaluable in guiding me and instilling a sense of self-critique in my work.

Despite my relatively brief time with the research group, I found these meetings to be highly enjoyable, and I always felt warmly welcomed. I want to extend my thanks to everyone who generously offered assistance and promptly addressed my inquiries. A special appreciation to Siënna Karremans for our collaboration and the intellectual exchanges we shared. Your input and discussions were greatly beneficial to this research.

I would like to extend my heartfelt gratitude to all those who contributed to the execution of the experiments. Special thanks to David Thompson, Rianne Bulthuis, Siënna Karremans, and Wilma Petersen for their valuable assistance and collaborative thinking during the experimental process. I am also deeply thankful to V. Trikalitis (MSc.) for his significant role in conducting and processing the TGA and DSC measurements.

Srirang, Rianne, David, Siënna, Wilma and Vasileios for your contributions have been indispensable, and I am genuinely thankful for the opportunity to work with each of you. This project would not have been possible without your support and guidance.

Finally, I would like to thank my friends and family for helping, inspiring, comfort and encouraging me. Without your love and support I would not have been able to finish this thesis.

References

[1] Sung H, Ferlay J, Siegel RL, Laversanne M, Soerjomataram I, Jemal A, et al. Global Cancer Statistics 2020: GLOBOCAN Estimates of Incidence and Mortality Worldwide for 36 Cancers in 185 Countries. CA Cancer J Clin. 2021 May;71(3):209-49. doi:10.3322/caac.21660.

[2] Zhou Y, Yao J, Wang LV. Tutorial on photoacoustic tomography. J Biomed Opt. 2016 Jun;21(6). doi:10.1117/1.JBO.21.6.061007.

[3] Manohar S, Dantuma M. Current and future trends in photoacoustic breast imaging. Photoacoustics. 2019 Dec;16. doi:10.1016/j.pacs.2019.04.004.

[4] PAM3: The 3rd Generation Photoacoustic-Ultrasound Imager; 2023. [Online; accessed 6. Sep. 2023]. Available from: https://www.utwente.nl/en/tnw/m3i/research/Photoacoustic

[5] PAMMOTH; 2021. [Online; accessed 6. Sep. 2023]. Available from: https://www.pammoth-2020.eu.

[6] Dantuma M, Dantuma M, van Dommelen R, Manohar S. Semi-anthropomorphic photoacoustic breast phantom. Biomed Opt Express. 2019 Nov;10(11):5921-39. doi:10.1364/BOE.10.005921.

[7] Maneas E, Xia W, Ogunlade O, Fonseca M, Nikitichev DI, David AL, et al. Gel wax-based tissue-mimicking phantoms for multispectral photoacoustic imaging. Biomed Opt Express. 2018 Mar;9(3):1151. doi:10.1364/BOE.9.001151.

[8] Hacker L, Joseph J, Ivory AM, Saed MO, Zeqiri B, Rajagopal S, et al. A Copolymer-in-Oil Tissue-Mimicking Material With Tuneable Acoustic and Optical Characteristics for Photoacoustic Imaging Phantoms. IEEE Trans Med Imaging. 2021 Jun;40(12):3593-603. doi:10.1109/TMI.2021.3090857.

[9] Boink Y. Data-driven reconstruction methods for photoacoustic tomography: Learning structures by structured learning [PhD Thesis - Research UT, graduation UT]. Netherlands: University of Twente; 2021. 30doi:10.3990/1.9789036550871.

[10] Technical Data – PA Imaging; 2023. [Online; accessed 9. Oct. 2023]. Available from: https://pa-imaging.com/en/technical-data.

[11] Oudry J, Bastard C, Miette V, Willinger R, Sandrin L. Copolymer-in-oil Phantom Materials for Elastography. Ultrasound Med Biol. 2009 Jul;35(7):1185-97. doi:10.1016/j.ultrasmedbio.2009.01.012.

[12] Polat K, Orujalipoor I, İde S, Sen M. Nano and microstructures of SEBS/PP/wax blend membranes: SAXS and WAXS analyses. Journal of Polymer Engineering. 2015 03;35. doi:10.1515/polyeng-2014-0093.

[13] Hacker L, Ivory AM, Joseph J, Gröhl J, Zeqiri B, Rajagopal S, et al. A Stable Phantom Material for Optical and Acoustic Imaging. JoVE (Journal of Visualized Experiments). 2023 Jun;(196):e65475. doi:10.3791/65475.

[14] Cabrelli LC, Sampaio DRT, Uliana JH, Carneiro AAO, Pavan TZ, de Ana AM. Copolymer-in-oil phantoms for photoacoustic imaging. In: 2015 IEEE International Ultrasonics Symposium (IUS). IEEE; 2015. p. 1-4. doi:10.1109/ULTSYM.2015.0395.

[15] Dantuma M. A hybrid multispectral photoacoustic-ultrasound breast imager: from the lab towards the clinic. Netherlands: University of Twente; 2021. 50doi:10.3990/1.9789036553049.

[16] Taroni P, Quarto G, Pifferi A, Abbate F, Balestreri N, Menna S, et al. Breast Tissue Composition and Its Dependence on Demographic Risk Factors for Breast Cancer: Non-Invasive Assessment by Time Domain Diffuse Optical Spectroscopy. PLoS One. 2015;10(6). doi:10.1371/journal.pone.0128941.

[17] Taroni P, Bassi A, Comelli D, Farina A, Cubeddu R, Pifferi A. Diffuse optical spectroscopy of breast tissue extended to 1100 nm. In: Journal of Biomedical Optics, Vol. 14, Issue 5. vol. 14. SPIE; 2009. p. 054030. doi:10.1117/1.3251051.

[18] Foschum F. Optical properties of gel wax phantoms. Institut für Lasertechnologien in der Medizin und Meßtechnik; 2022.

[19] Nebeker J, Nelson TR. Imaging of Sound Speed Using Reflection Ultrasound Tomography. J Ultrasound Med. 2012 Sep;31(9):1389-404. doi:10.7863/jum.2012.31.9.1389.

[20] Sandhu GYS, Li C, Roy O, West E, Montgomery K, Boone M, et al. Frequency-domain ultrasound waveform tomography breast attenuation imaging. In: Proceedings Volume 9790, Medical Imaging 2016: Ultrasonic Imaging and Tomography. vol. 9790. SPIE; 2016. p. 93-104. doi:10.1117/12.2218374.

[21] Lee JY, An J, Chua CK. Fundamentals and applications of 3D printing for novel materials. Appl Mater Today. 2017 Jun;7:120-33. doi:10.1016/j.apmt.2017.02.004.

[22] Gill P, Moghadam TT, Ranjbar B. Differential Scanning Calorimetry Techniques: Applications in Biology and Nanoscience. Journal of Biomolecular Techniques : JBT. 2010 Dec;21(4):167. Available from: https://www.ncbi.nlm.nih.gov/pmc/articles/PMC2977967.

[23] Crist B. Thermodynamics of statistical copolymer melting. Polymer. 2003 Jul;44(16):4563-72. doi:10.1016/S0032-3861(03)00331-8.

[24] ; 2021. [Online; accessed 30. Oct. 2023]. Available from: https://resources.perkinelmer.com/lab-solutions/resources/docs/faq$_b eginners - guide - to - thermogravimetric - analysis_0$09380$c_0$1.$pdf$.

[25] Dantuma M, Lucka F, Kruitwagen SC, Javaherian A, Alink L, van Meerdervoort RPP, et al. Fully three-dimensional sound speed-corrected multi-wavelength photoacoustic breast tomography. arXiv. 2023 Aug. doi:10.48550/arXiv.2308.06754.

[26] Mäntele W, Deniz E. UV–VIS absorption spectroscopy: Lambert-Beer reloaded. Spectrochim Acta, Part A. 2017 Feb;173:965-8. doi:10.1016/j.saa.2016.09.037.

[27] Xia W, Piras D, van Hespen JCG, Steenbergen W, Manohar S. A new acoustic lens material for large area detectors in photoacoustic breast tomography. Photoacoustics. 2013 May;1(2):9-18. doi:10.1016/j.pacs.2013.05.001.

[28] View of Understanding Archimedes Law: What the Best Teaching Strategies for Vocational High School Students with Hearing Impairment; 2023. [Online; accessed 14. Oct. 2023]. Available from: https://publisher.uthm.edu.my/ojs/index.php/JTET/article/view/5399/3535.

[29] Hacker L. Privécommunication; 2023. University of Oxford. Personal communication.

List of Figures

List of Tables

List of Acronyms

3D	Three-dimensional
PA	Photoacoustic
US	Ultrasound
SEBS	Styrene-ethylene/butylene-styrene
LDPE	Low-density Polyethylene
TiO_2	Titanium dioxide
SBS	Styrene-butadiene-styrene
BMI	Body Mass Index
IAD	Inverse Adding-doubling
DSC	Differential scanning calorimetry
T_g	Glass transition temperature
T_m	Melting temperature
T_d	Decomposition temperature
TGA	Thermogravimetric analysis
rpm	revoltions per minute
FWHM	Full width at half maximum

List of Acronyms

Symbol	Unit	Definition
$H(r)$	$Jm^{-3}s^{-1}$	Absorbed optical energy
$p_0(r)$	Pa	Initial pressure
$\phi(r)$	Jcm^{-2}	Light fluence
μ_a	cm^{-1}	Absorption coefficient
Γ	-	Grüneisen coefficient
β	K^{-1}	Isobaric thermal expansion coefficient
c_s	m/s	Speed of sound of the sample
C_p	$Jkg^{-1}K^{-1}$	Isobaric specific heat capacity
$\mu_s^{'}$	cm^{-1}	Reduced scattering coefficient
α	$dB/(mmMHz)$	Acoustic attenuration coefficient
M_R	-	Total reflection
M_T	-	Total transmission
λ	nm	Wavelength

Appendix

A Materials

Table 8 is an overview of the used materials.

Table 8: A list of the used materials

Name	Company	Detail	Comments
Mineral oil	Sigma-Aldrich	8042-47-5	0.833 g/ml
LDPE	Sigma-Aldrich	9002-88-4	
SEBS	Sigma-Aldrich	66070-58-4	0.91 g/ml
Yellow wax	Rayher		From Bertus Workel in Enschede
Personal safety equipment			Lab coat, gloves and glasses
Fume hood	Waldner	Secuflow-abzug	
sonicator bath	Bransonic	Z245143	Ultrasonic cleaner
Heat transfer fluid	Petro-Canada	CALFLO HTF	0003 BATCH# 164032
Oil bath	IKA	IKA HBR 4 control	
Vacuum oven	HERAEUS	VT5042 EK vacuüm oven	
Vacuum pump	Value tool	V-i120SV	
Heat-resistant gloves	MAPA prfessional	TempTec 332	
Metal spatulas			
Overhead stirrer	IKA	IKA RW 16 basic	Z403903-1EA
Analytical balance scale	Sartorius	BP210D	
UV-VIS spectrophotometer	SHIMADZU	UV-2600	
Non-adhesive spray	Vosschemie	Trennspray Voss loswas 400gr	
Pulse receiver	Panametrics	Model 5077PR	
US transducers	Olympius panametrics	V303, V306 and V309	1, 2.25 and 5 MHz
Needle Hydrophone	Precision Acoustics	SN 1887	1mm
Pre amplifier	Precision Acoustics	Submersible preamplifier	
DC coupler	Precision Acoustics		With power supply
PC-oscilloscope	PicoScope	2000 series	
Oscilloscope	Tektronix	TDS 2024C	
Thermocouple	National instruments	Type k	
Water bath			With water from the tap
PC			With PicoScope 7 software

B Copolymer-in-oil protocol

The required materials are shown in Table 8 in Appendix A. For making the copolymer-in-oil, the following protocol should to be followed. The copolymer-in-oil is made on 19-10-2023 with Siënna Karremans. The protocol is based on Hacker2023 [13].
12 w/w% SEBS, 5 w/w% LDPE, 0.03 w/w% yellow wax

Table 9: The components for the stock solution to get 3.03 w/w% yellow wax, 96.97 w/w% mineral oil

	w/w%	Density (g/ml)	Volume (ml)	Amount (g)	Weighed
Mineral oil	96.97	0.833	40	33.22	33.21/33.22 g
Yellow wax	3.03			1.038	1038.0 mg
Total	100			34.248	34.248 g

Table 10: The components for the copolymer-in-oil to get 12 w/w% SEBS, 5 w/w% LDPE, 0.03 w/w% yellow wax

	w/w%	Density (g/ml)	Volume (ml)	Amount (g)	Weighed (g)
Mineral oil	82	0.833	750	624.750	624.75
SEBS	12	0.91		91.427	81.18+10.25 = 91.429
LDPE	5			38.095	38.10
Stock solution	1			7.61	7.63
Total	100			761.890	762.909

Stock solution

1. Add 33.21 g mineral oil and 1038.0 mg yellow wax (Rayher) to each other. First the mineral oil in the tube and then the wax.
2. Rocked back and forth briefly and then into the sonicator bath, see Figure 20a.
   (a) Duration: 15+24 = 39 min
   (b) Begin temperature: 55 °celcius
   (c) T(15) = 54
   (d) End temperature: 52 °celsius
3. See Figure 20b.
4. From this stock solution s 7.63 g in another tube.

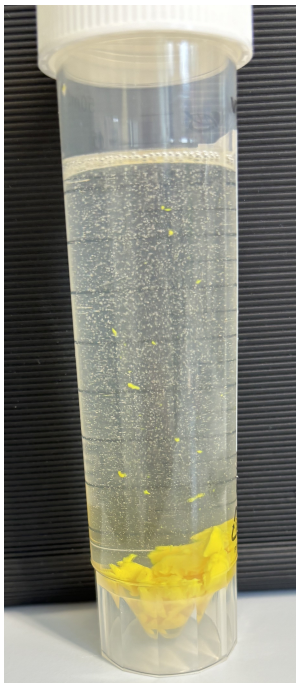

(a) The stock solution before entering the sonicator bath

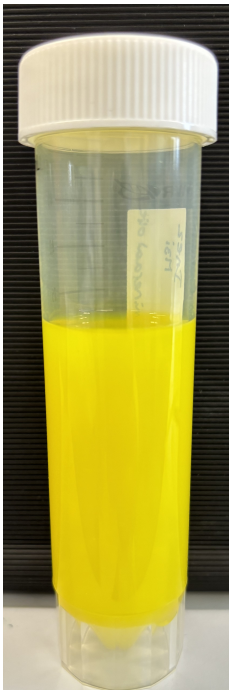

(b) The stock solution after the sonicator bath

Figure 20: The stock solution

Copolymer-in-oil

1. All the materials are weighed
   (a) SEBS: first 81.18 g from the first jar, which then ran out so even later 10.25 was added
   (b) Mineral oil: also from two different bottles
2. Add all components together in a beaker
   (a) Mineral oil
   (b) LDPE
   (c) SEBS → properly use a spoon to remove the leftovers from the beaker
   (d) Stock solution
3. See the components of the copolymer in oil before entering the oil bath in Figure 21

Figure 21: The copolymer-in-oil components before entering the oil bath

Oil bath

1. Setup, see Figure 22b: 1 bar with mechanical stirrer, 2 bar with tyreps
2. Oil bath is heated up to 150 °C
3. Rotation per minute: 150 rpm
4. Put the beaker glass in the oil bath using the setup (see Figure 22a)
5. Mechanical sirrer → first on 1, then slowly to 4
6. Duration: 1 hour and 22 minutes

    (a) Look good if all the components are dissolved and mixed completely, Figure 5

After about 1 hour and 8 minutes the mechanical stirrer is turned off, this way no more air bubbles are being formed, but it will be melted.

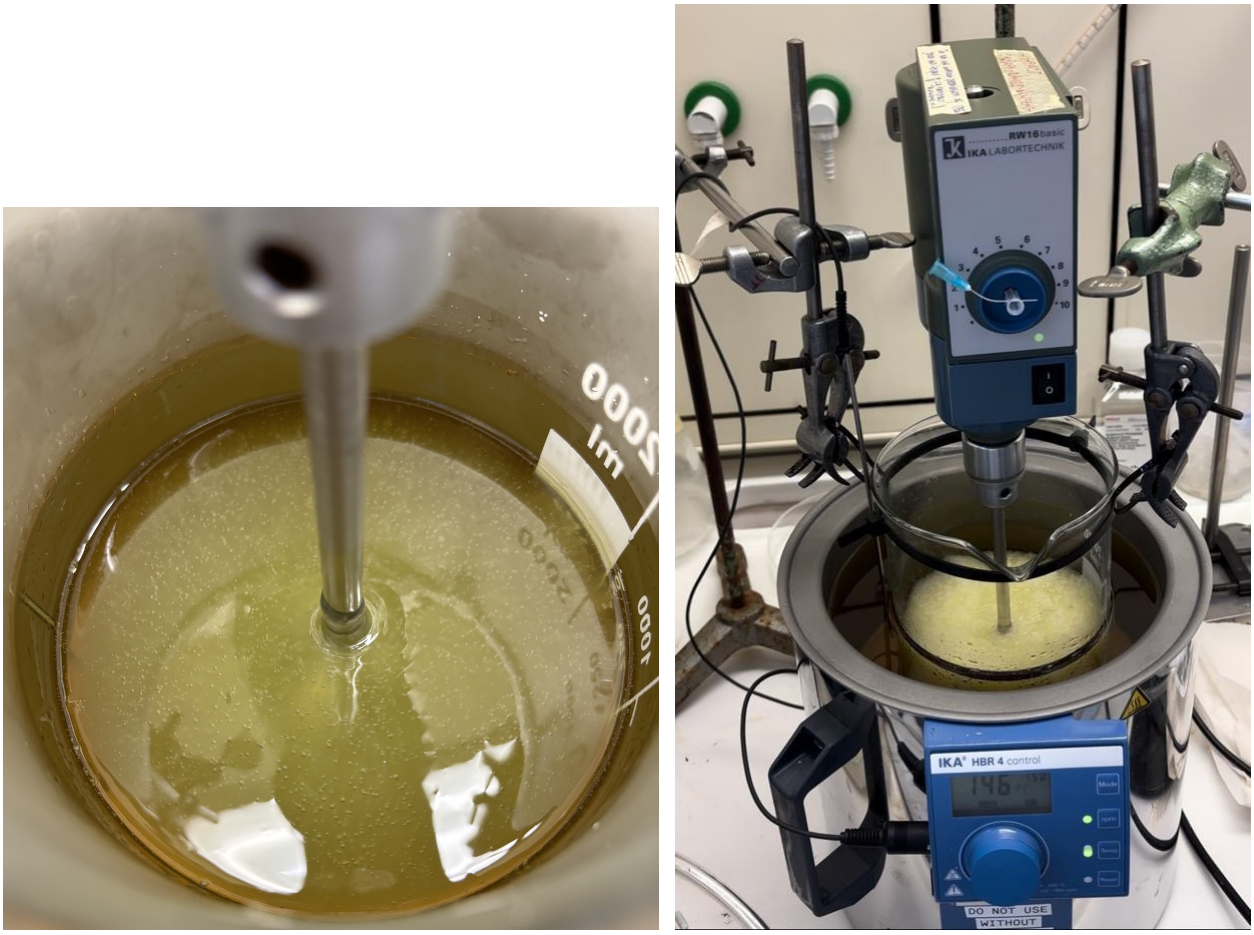

(a) The copolymer-in-oil in the oil bath, this is at about 1 hour in.

(b) The beaker glass in the oil bath at the beginning of the heating process

Figure 22: The copolymer-in-oil in the oil bath

Vacuum

1. Preheat the oven to 150 degrees
2. Put the beaker glass in the oven
3. Set the vacuum pomp on
4. See Figure 23 at about 45 minutes in the oven
5. Duration: 1 hour and 20 min

    (a) Look good if all the air bubbles have been removed

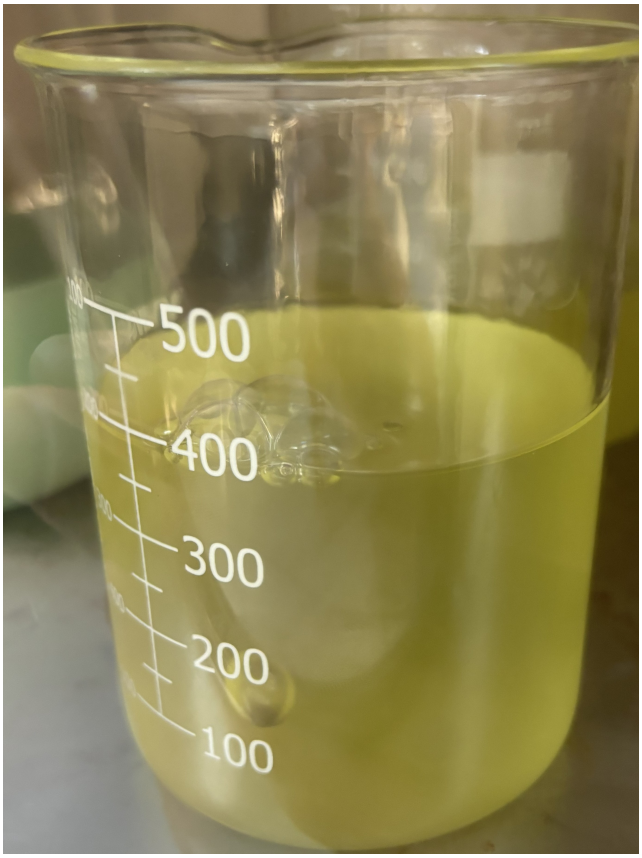

Figure 23: The copolymer-in-oil in the vacuum oven

Mould

1. Clean all the moulds the are going to be used
2. Spray them with non adhesive
3. Pour them solowly
4. See Figure 24a and 24bfor the end results

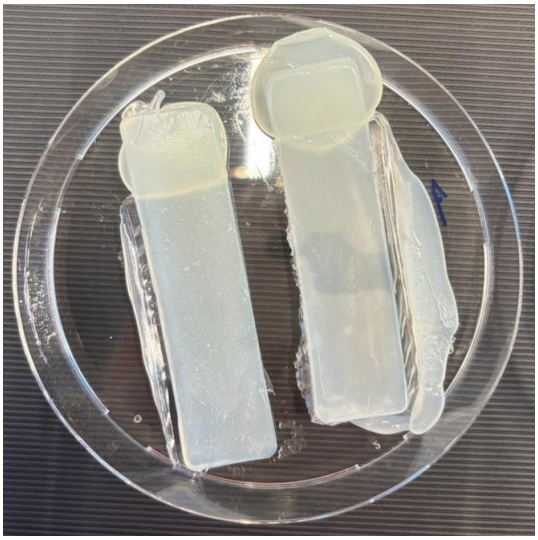

(a) The copolymer-in-oil samples arrived with the spacers for the optical measurements.

(b) the copolymer-in-oil in a cube for the acoustic measurements

Figure 24: The stock solution

C Protocol for optical properties

Thickness of samples

Table 11: Thickness of the different samples used for the IAD measurements.

Sample	1 (mm)	2 (mm)	3 (mm)	Mean (mm)
A1	2.98	3.30	3.11	3.13
A2	3.10	3.18	3.06	3.11
B1	2.91	2.89	2.88	2.89
B2	2.91	2.93	2.89	2.91

IAD setup

1. Start PC
2. Open UV-probe software
3. Start spectrophotometer
4. Connect with spectrophotometer in software
5. Set all settings by M
   (a) Wavelength range (nm): 1100-450
   (b) Scan speed: Medium
   (c) Interval(nm): 1.0
   (d) Threshold: 100
   (e) Points: 100
   (f) Measuring mode: reflectance/transmittance. In this case Reflectance.
   (g) Detector unit: external(2Detectors)
   (h) Slit width (nm): 5.0
   (i) Light source change wavelength: 320 nm
   (j) Detector change wavelength: 900 nm
   (k) S/R exchange: normal
   (l) Accumulation: 2.0
   (m) Stair correction: on
6. See Figure 25 for inside spectrophotometer
   (a) Arm 1: nothing
   (b) Arm 2: noting
   (c) Arm 3: block beam
   (d) Arm 4: block beam
7. Start baseline from 1100-450 nm
8. $M \rightarrow$ measuring mode: Transmittance
9. $T0 \rightarrow$ same as baseline
10. $Tdark \rightarrow$ block beam in arm 2
11. $Tstd\_1 \rightarrow$ standard sample (thick) in arm 2
12. $Tstd\_2 \rightarrow$ standard sample (thin) in arm 2
13. $M \rightarrow$ Measuring mode: Reflectance
14. $R0 \rightarrow$ arm 2 nothing, arm 3 nothing
15. $Rstd\_1 \rightarrow$ standard sample (thick) in arm 3
16. $Rstd\_2 \rightarrow$ standard sample (thin) in arm 3

Figure 25: The inside of the spectrophotometer, with the names of the different arms.

IAD measuring

1. $M \rightarrow$ Same as 5 & 6 from IAD setup
2. $M \rightarrow$ Measuring mode: Transmittance
3. $Ts\_A1\_1 \rightarrow$ Sample A1 in arm 2
4. $Ts\_A1\_2 \rightarrow$ Turn the sample in arm 2
5. Ts_A2_1, Ts_A2_2, Ts_B1_1, Ts_B1_2, Ts_B2_1, $Ts\_B2\_2 \rightarrow$ same as 3 & 4
6. $M \rightarrow$ Measuring mode: Reflectance
7. Arm 2 empty
8. $Rs\_A1\_1 \rightarrow$ Sample A1 in arm 3
9. $Rs\_A1\_2 \rightarrow$ Turn the sample in arm 3
10. Rs_A2_1, Rs_A2_2, Rs_B1_1, Rs_B1_2, Rs_B2_1, $Rs\_B2\_2 \rightarrow$ same as 3 & 4
11. Save all data in UV probe
12. Save all raw data in excel $\rightarrow$ notes and then control A, control C and control V in excel

Comments:

- 11 & 12 can also be done during the waiting time from the measurements.
- When taking out the samples, the sample was stuck to the plastic. So a really thin layer remained behind. See Figure 26.
- The IAD method did not seem to be the right analyse method, so only Ts was used for the anlysis.

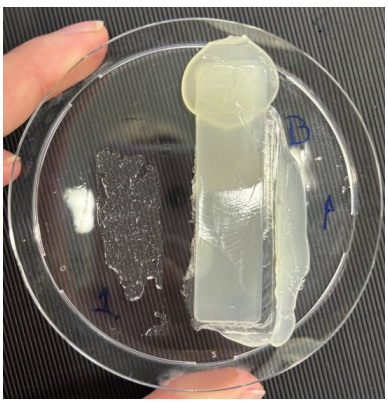

Figure 26: The remaining layer in the tray.

D Matlab for optical characterization

Matlab for absorption coefficient For sample A1

```
%20-10-2023

clear all, clc, close all

%cd '\\ad.utwente.nl\TNW\M3I\Users\Inez Nijhof\Code\Optical characterization\IAD-20-10\iad-win-3-12-0' % adjust to file path of... installed IAD program
filepath = '\\ad.utwente.nl\TNW\M3I\Users\Inez Nijhof\Data\optical characterization\20-10-2023\20231020_Ci0.xlsx'; % adjust to file ... path of measured data
data = xlsread(filepath);

%% define data columns
wl_data = data(:,1);

T00 = data(:,2);
Tdark = data(:,3);
R00 = data(:,6);

%% the values of the sample, choose one of the three options, ... measurement 1 or 2 or mean
Ts= data(:,11); % mean of Ts_A1_1 and Ts_A1_2
Rs = data(:,23); % mean of Rs_A1_1 and Rs_A1_2

% Ts = data(:, 9); %Ts_A1_1
% Rs= data(:, 21); %Rs_A1_1
%
% Ts = data(:, 10); %Ts_A1_2
% Rs= data(:, 22); %Rs_A1_2

%% transmission % convertion to absorption coefficient
T= Ts/100; % transmittance
d = 3.13e-1; %thickness of the cuvet is 1 cm
A= -log10(T); %absorbance
mu_a = A/d; % absorption coefficient

%% plot mua
figure()
plot(wl_data, mu_a)

xlabel('wavelength (nm)')
ylabel('Absorption coefficient (cm^{-1})')
title('The absorption coefficient by wavelength of the mean of Ts\_A1\..._1 and Ts\_A1\_2')



%% literature
filepath = '\\ad.utwente.nl\TNW\M3I\Users\Inez Nijhof\Data\optical characterization\literature.xlsx'; % adjust to file path of ... measured data
data_lit = xlsread(filepath);


```

```
%% define data columns
wl_data_lit_adipose = data_lit(:,1);
wl_data_lit_Fibrous = data_lit(:,4);

mua_lit_adipose = data_lit(:,2);
mua_lit_fibrous = data_lit(:,5);

%% add to figure
hold on
plot(wl_data_lit_Fibrous, mua_lit_fibrous)
plot(wl_data_lit_adipose, mua_lit_adipose)
hold off
legend('Copolymer-in-oil', 'Taroni2009 fibrous', 'Taroni2009 adipose')
```

E Protocol for acoustic properties

26-10-2023 Acoustic characterization
Transducer: 1MHz

Table 12: The raw data of the speed of sound measurements with the 1MHz transducer

Length	d1= 49.12 mm	t= 48.52 µs	T=22.9 °C
Width	d2= 35.09 mm	t= 48.2 µs	T=22.9 °C
Water	d= 63 mm	t= 47.7 µs	T=22.9 °C

Settings in picoscope 7:

- A= ±50 mV
- B= ±5 V
- Sample freq: 25 MS/s
- Trigger: bron A, 9mV
- Samples: 2500s
- Scope: 10 µs/div

The measurements were done with a pulser voltage of 100 V.

Transducer: 2.25MHz

Table 13: The raw data of the speed of sound measurements with the 2.25MHz transducer

Length	d1= 49.07 mm	t= 43.95 µs	T=22.8 °C
Width	d2= 34.63 mm	t= 43.57µs	T=22.8 °C
Water	d= 66 mm	t= 43.07 µs	T=22.8 °C

Settings in picoscope 7:

- A= ±200 mV
- B= ±5 V
- Sample freq: 25 MS/s
- Trigger: bron A, 9mV
- Samples: 2500s
- Scope: 10 µs/div

The measurements were done with a pulser voltage of 100 V.

Transducer: 5MHz

Table 14: The raw data of the speed of sound measurements with the 5MHz transducer

Length	d1= 49.25 mm	t= 35.44 µs	T=22.7 °C
Width	d2= 34.45 mm	t= 35.20 µs	T=22.7 °C
Water	d= 66 mm	t= 42.31 µs	T=22.7 °C

Settings in picoscope 7:

- A= ±200 mV
- B= ±5 V
- Sample freq: 25 MS/s

- Trigger: bron A, 9mV
- Samples: 2500s
- Scope: 10 µs/div

The measurements were done with a pulser voltage of 400 V.

Protocol:

1. Make the set up, based on Figure 9
   (a) Connect the pulser receiver, T/R, to the transducer 1MHz.
   (b) Connect the hydrone needle to the preamplifier.
   (c) Connect the preamplifier to the DC coupler.
   (d) At the output of the DC coupler connect a T connection.
      i. Connect to one end of the T connection the oscilloscope.
      ii. Connect to the other end of the T connection the picoscope.
   (e) At the sync out of the pulser receiver, connect a T connection.
      i. Connect to one end of the T connection the oscilloscope.
      ii. Connect to the other end of the T connection the picoscope.
   (f) Connect the picoscope to a PC with the picoscope 7 software.
   (g) Connect a thermocouple to the PC.
   (h) Connect the transducer, hydrophone needle and the sample to a rails.
   (i) Put the rails into a container with water. See Figure 27.
   (j) Put the end of the thermocouple in the water as well.
2. Turn on the oscilloscope, pulser receiver and DC coupler.
3. Set the setting of the picoscope 7 software according to the above settings for the 1MHz transducer.
4. Safe the data of d1.
   (a) The 'huidig' wave as a MATLAB file.
   (b) All waves as a PS 'gegevens'file.
5. Turn the sample to derive d2.
6. Save the data of d2.
   (a) The 'huidig' wave as a MATLAB file.
   (b) All waves as a PS 'gegevens'file.
7. Remove the sample.
8. Save the data of d.
   (a) The 'huidig' wave as a MATLAB file.
   (b) All waves as a PS 'gegevens'file.
9. Take out the rails with the transducer and the hydrophone needle.
10. Measure the distance between the transducer and hydrophone needle.
11. Change the transducer to 2.25 MHz.
12. Preform step 1h to 10 for the second transducer.
13. Change the transducer to 5 MHz.
14. Preform step 1h to 10 for the third transducer.

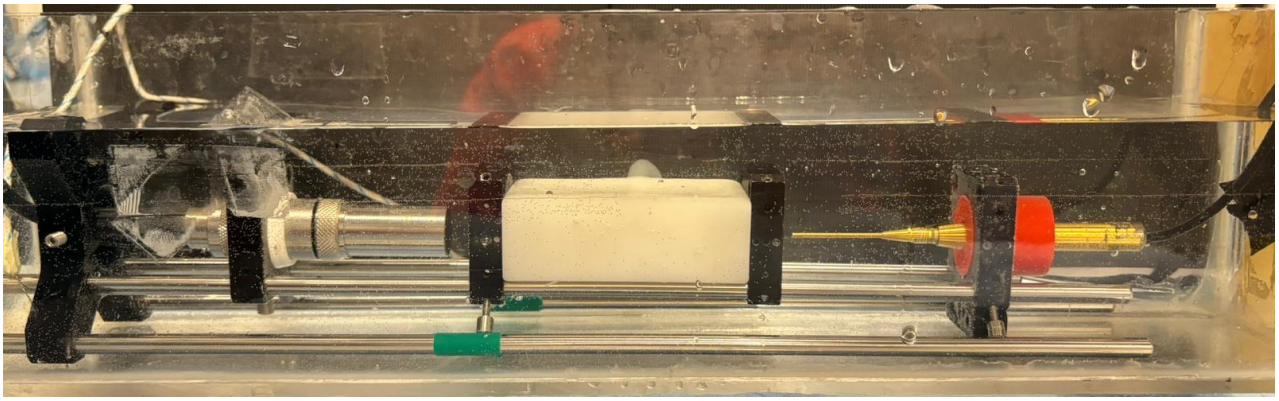

Figure 27: The transducer, sample and hydrophone needle in the container with water.

F Equation speed of sound

The derivation of equation 6 is given below.

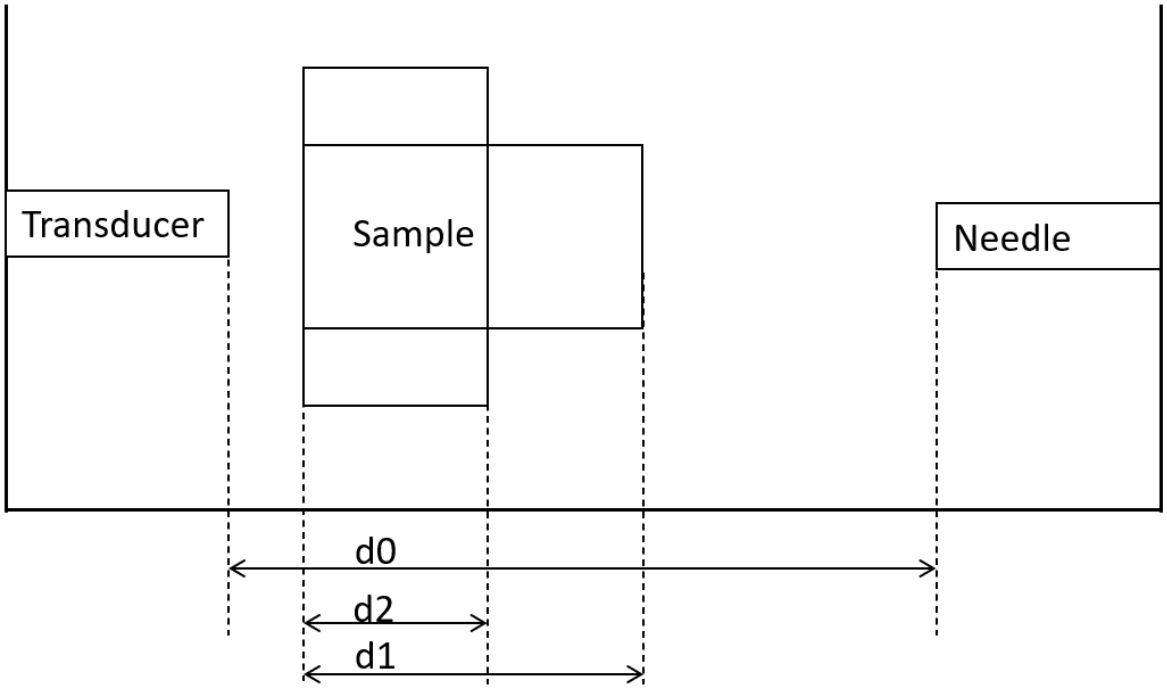

Figure 28: Schematic overview of values to derive the speed of sound equation.

$$t_0 = \frac{d_0}{C_w} \tag{F1}$$

$$t_1 = \frac{d_0 - d_1}{C_w} + \frac{d_1}{C_s} \tag{F2}$$

$$t_2 = \frac{d_0 - d_2}{C_w} + \frac{d_2}{C_s} \tag{F3}$$

$$\Delta d = d_2 - d_1 \tag{F4}$$

$$\Delta t = t_2 - t_1 \tag{F5}$$

$$\Delta t = \frac{d_0 - d_2}{C_w} + \frac{d_2}{C_s} - \frac{d_0 - d_1}{C_w} - \frac{d_1}{C_s} \tag{F6}$$

$$\Delta t = \frac{d_0 - d_2 - d_0 + d_1}{C_w} + \frac{d_2 - d_1}{C_s} \tag{F7}$$

$$\Delta t = \frac{-d_2 + d_1}{C_w} + \frac{d_2 - d_1}{C_s} \tag{F8}$$

$$\Delta t = \frac{-\Delta d}{C_w} + \frac{\Delta d}{C_s} \tag{F9}$$

$$\frac{\Delta d}{C_s} = \Delta t + \frac{\Delta d}{C_w} \tag{F10}$$

$$\Delta d = C_s(\Delta t + \frac{\Delta d}{C_w}) \tag{F11}$$

$$C_s = \frac{\Delta d}{(\Delta t + \frac{\Delta d}{C_w})} \tag{F12}$$

G Matlab for speed of sound

Function speed of sound of water

```
function c = speedSoundWater(T)
%SPEEDSOUNDWATER   Calculate the speed of sound in water with ... temperature.
%
% DESCRIPTION:
%       speedSoundWater calculates the speed of sound in distilled ... water at
%       a given temperature using the 5th order polynomial given by
%       Marczak.
%
% USAGE:
%       c = speedSoundWater(T)
%
% INPUTS:
%       T   - water temperature [degC]
%
% OUTPUTS:
%       c   - speed of sound [m/s]
%
% ABOUT:
%       author: Bradley E. Treeby
%       date: 11th August 2008
%       reference: Marczak (1997) "Water as a standard in the ... measurements
%       of speed of sound in liquids," J. Acoust. Soc. Am., 102, ... 2776-2779
%
% This function is part of the k-Wave Toolbox (http://www.k-wave.org)
% Copyright (C) 2009-2014 Bradley Treeby and Ben Coxx

% This file is part of k-Wave. k-Wave is free software: you can
% redistribute it and/or modify it under the terms of the GNU Lesser
% General Public License as published by the Free Software Foundation,
% either version 3 of the License, or (at your option) any later ... version.
%
% k-Wave is distributed in the hope that it will be useful, but ... WITHOUT ANY
% WARRANTY; without even the implied warranty of MERCHANTABILITY or ... FITNESS
% FOR A PARTICULAR PURPOSE.  See the GNU Lesser General Public License... for
% more details.
%
% You should have received a copy of the GNU Lesser General Public ... License
% along with k-Wave. If not, see <http://www.gnu.org/licenses/>.

p(1) = 2.787860e-9;
p(2) = -1.398845e-6;
p(3) = 3.287156e-4;
p(4) = -5.779136e-2;
p(5) = 5.038813;
p(6) = 1.402385e3;
c = polyval(p, T);
```

Acoustic characterization

```
%% Determine speed of sound and acoustic attenuation test blocks
% Based on a script by Maura Dantuma, 25-9-2018

clear all, close all
clc

cd '\\ad.utwente.nl\TNW\M3I\Users\Inez Nijhof\Code\Acoustic characterization\26-10-2023'

sample = 'sample1';
d1 = 34.72e-3;
d2 = 49.15e-3;
dblock = d1-d2; %m ; difference in thickness between d1 and d2
watersos = speedSoundWater(22.8); % input is temperature in degrees Celsius
max_L = 8001;

%% Read data transmission
soundspeeds_peak =[];
soundspeeds_threshold = [];
F = [];
attenuation = [];
attenuation2 = [ ];
frequencies = [1 2.25 5];

for i=1:length(frequencies);
    filename = ['20231026-', sample, '_d1_', num2str(frequencies(i)), 'MHz.mat'];
    cd '\\ad.utwente.nl\TNW\M3I\Users\Inez Nijhof\Data\Acoustic characterization\26-10-2023\'
    load(filename);
    V_d1=A;
    filename = ['20231026-', sample, '_d2_', num2str(frequencies(i)), 'MHz.mat'];
    load(filename);
    V_d2=A;
    t = linspace(0,2504*Tinterval,2504);
    cd '\\ad.utwente.nl\TNW\M3I\Users\Inez Nijhof\Data\Acoustic characterization\26-10-2023\'
    figure(1);
    subplot(length(frequencies),1,i);
    hold all
    plot(t(1:length(V_d1)),V_d1,'k');
    plot(t(1:length(V_d2)),V_d2,'k--');
    %insert correct block name in title
    sgtitle('Sample 1: US signal over time measured at three different frequencies')
    title([num2str(frequencies(i)), 'MHz']);
    ylabel('Voltage (V)')
    xlabel('Time (s)')
    legend('d1', 'd2')
    xlim([2e-5,5.3e-5])

    L=length(t); %length measured signals
```

```
48      dt = Tinterval;
49      Fs=1/dt;
50
51      threshold = 0.05;
52      tthreshold_d1= find(V_d1 > threshold, 1)*Tinterval;
53      tthreshold_d2= find(V_d2 > threshold, 1)*Tinterval;
54      Vthreshold_d1= V_d1(tthreshold_d1/Tinterval);
55      Vthreshold_d2= V_d2(tthreshold_d2/Tinterval);
56
57
58
59      [Vpeak_d1,tpeak_d1]=(max(V_d1));
60      [Vpeak_d2,tpeak_d2]=(max(V_d2));
61      figure(1);
62      subplot(length(frequencies),1,i);
63      hold all
64      plot(t(tpeak_d1),Vpeak_d1,'go','MarkerSize',5);
65      plot(t(tpeak_d2),Vpeak_d2,'go','MarkerSize',5);
66      plot(tthreshold_d1,Vthreshold_d1,'ro','MarkerSize',5);
67      plot(tthreshold_d2,Vthreshold_d2,'ro','MarkerSize',5);
68      legend('d1', 'd2', 'peak d1', 'peak d2', 'threshold d1', '...
            threshold d2')
69      %selecting only the pulse itself
70      ind_peak = find(V_d1 == Vpeak_d1);
71      %calculate sound speeds from peaks
72      c_peak = dblock/((tpeak_d1-tpeak_d2)*dt+(dblock/watersos));
73      soundspeeds_peak = [soundspeeds_peak,c_peak];
74      cmean_peak = mean(soundspeeds_peak);
75
76      %calculate sound speeds from threshold
77      c_threshold = dblock/((tthreshold_d1-tthreshold_d2)+(dblock/...
            watersos));
78      soundspeeds_threshold = [soundspeeds_threshold,c_threshold];
79      cmean_threshold = mean(soundspeeds_threshold);
80
81      % zeropadding
82      added_length = max_L - length(V_d1);
83      V_d1_f = [V_d1, zeros(1,added_length)];
84      V_d2_f = [V_d2, zeros(1,added_length)];
85      t_f = 0:dt:dt.*(max_L-dt);
86      V_d1_f = V_d1_f(1:2000);
87      V_d2_f = V_d2_f(1:2000);
88      t_f = t_f(1:2000);
89      [¬,tpeak_d1]=(min(V_d1_f));
90      [¬,tpeak_d2]=(min(V_d2_f));
91
92
93
94      % calculating the attenuation in dB/cm
95      att=20*log10((Vpeak_d1)/(Vpeak_d2))/(dblock.*1e2);
96      attenuation = [attenuation, att]; % simple attenuation calculation
97
98      % applying a gaussian filter to filter out the noise
99      V_d1_f=V_d1_f.*exp((-(t_f-t_f(tpeak_d1)).^2)/(5*(1e-6^2)));
100     V_d2_f=V_d2_f.*exp((-(t_f-t_f(tpeak_d2)).^2)/(5*(1e-6^2)));
101     % figure(2); subplot(length(frequencies),1,i); hold all
102     % plot(t_f,V_d1_f,'k');
103     % plot(t_f,V_d2_f,'k--');
104     % xlim([0.6e-4,0.8e-4])
```

```
105
106     % attenuation from fourier transform
107     L=length(t_f);
108     figure(); subplot(length(frequencies),1,i); hold all
109     Ad1=fft(V_d1_f(1:end-1));
110     P2=abs(Ad1/L);
111     Ad1=P2(1:(L/2)+1);
112     Ad1(2:end-1)=2*Ad1(2:end-1);
113     f=Fs*(0:(L/2))/L;
114     plot(f,Ad1);
115     Ad2=fft(V_d2_f(1:end-1));
116     P2=abs(Ad2/L);
117     Ad2=P2(1:(L/2)+1);
118     Ad2(2:end-1)=2*Ad2(2:end-1);
119     plot(f,Ad2);
120     legend('d1', 'd2')
121     xlim([0 10e6]);
122
123     %selecting the lower and upper frequency bounds of the region you ...
            want to analyze
124     [x,y] = ginput(2);
125     [~,ind_ll]=min(abs(f-x(1)));
126     [~,ind_ul]=min(abs(f-x(2)));
127     % calculating attenuation in dB/cm from these selected regions
128     att2=20.*log10((Ad1(ind_ll:ind_ul)./Ad2(ind_ll:ind_ul)))./(dblock...
            .*1e2);
129     attenuation2 = [attenuation2, att2]; % attenuation calculation
130
131
132     figure(); hold all
133     plot((f(ind_ll:ind_ul)*(10^-6)),att2) %10^-6 added to go back to ...
            MHz range so that correct values in power law are obtained
134     xlabel('Frequency (MHz)')
135     ylabel('Attenuation coefficient (dB/cm)')
136     title('Sample 1: acoustic attenuation coefficient over frequency')...
            %insert correct block name in title
137
138     F = [F f(ind_ll:ind_ul)];
139
140 end
141
142
143 %% curve fitter tool --> to matlab code
144 function [fitresult, gof] = createFit(F, attenuation2)
145 %CREATEFIT(F,ATTENUATION2)
146 %  Create a fit.
147 %
148 %  Data for 'untitled fit 1' fit:
149 %      X Input: F
150 %      Y Output: attenuation2
151 %  Output:
152 %      fitresult : a fit object representing the fit.
153 %      gof : structure with goodness-of fit info.
154 %
155 %  See also FIT, CFIT, SFIT.
156
157 %  Auto-generated by MATLAB on 27-Oct-2023 10:33:33
158
159
```

```
%% Fit: 'untitled fit 1'.
[xData, yData] = prepareCurveData( F, attenuation2 );

% Set up fittype and options.
ft = fittype( 'poly1' );

% Fit model to data.
[fitresult, gof] = fit( xData, yData, ft );

% Plot fit with data.
figure( 'Name', 'untitled fit 1' );
h = plot( fitresult, xData, yData );
legend( h, 'attenuation2 vs. F', 'untitled fit 1', 'Location', '...
    NorthEast', 'Interpreter', 'none' );
% Label axes
xlabel( 'F', 'Interpreter', 'none' );
ylabel( 'attenuation2', 'Interpreter', 'none' );
grid on
end
```